Russian Chemical Reviews **82** (5) 465 – 482 (2013) © 2013 Russian Academy of Sciences and Turpion Ltd

DOI 10.1070/RC2013v082n05ABEH004325

Metal nanoparticles in catalytic polymer membranes and ion-exchange systems for advanced purification of water from molecular oxygen

V V Volkov, T A Kravchenko, V I Roldughin

Contents

I.	Introduction	465
II.	Synthesis of nanoparticles	466
III.	Catalytic polymer membranes	471
IV.	Nanocomposites based on ion-exchange materials	472
V.	Membrane methods of oxygen reduction	474
VI.	Oxygen reduction in ion-exchange systems	476

Abstract. Methods of synthesis of metal nanoparticles and metal/polymer nanocomposites including ion-exchange materials are considered. The effect of the composition and size of nanoparticles on their catalytic activity is analyzed. Attention is focused on the composites used in catalytic processes, namely, catalytic membranes and ion-exchange systems. The problems associated with the removal of dissolved oxygen from water by means of such composites are discussed. The bibliography includes 225 references.

I. Introduction

Dissolved oxygen is always present in aqueous and non-aqueous media that are in contact with the atmosphere. Molecular oxygen (dioxygen) is a reactive chemical in particular, a strong oxidant. For example, the action of oxygen is responsible for corrosive destruction of metals and alloys the corrosion protection of which has been a central problem for many years. Moreover, due to its reactivity, oxygen often represents a competitive impurity that has an adverse effect on many industrial processes. For this very reason, modern technologies have to use high-purity water.

V V Volkov A V Topchiev Institute of Petrochemical Synthesis, Russian Academy of Sciences, Leninsky prosp. 29, 119991 Moscow, Russian Federation. Tel. (7-495) 258 53 17, e-mail: vvvolkov@ips.ac.ru
T A Kravchenko Voronezh State University, Universitetskaya pl. 1, 394006 Voronezh, Russian Federation. Tel. (7-473) 220 85 38, e-mail: krav280937@yandex.ru
V I Roldughin A N Frumkin Instiute of Physical Chemistry and Electrochemistry, Russian Academy of Sciences, Leninsky prosp. 31, 119071 Moscow, Russian Federation; Department of Chemistry, Moscow State University, Leninskie Gory 1, 119991 Moscow, Russian Federation. Tel. (7-495) 955 46 47, e-mail: roldugin@phyche.ac.ru

Received 27 April 2012
Uspekhi Khimii **82** (5) 465 – 482 (2013); translated by T Ya Safonova

Decreasing the content of dissolved oxygen is an important stage of pretreatment of process water used in large-scale industries such as microelectronics, oil and gas industry (injected water), food industry, thermal and nuclear power engineering. The concentration of dissolved oxygen in water under ambient conditions is 8 mg kg^{-1}. Meanwhile water meant, for instance, for nuclear power stations and microelectronics should not contain more than 7 – 10 and 1 μg kg^{-1} of oxygen, respectively.

The physical, chemical, electrochemical and sorption methods of oxygen removal from liquid and gaseous media are well known. The conventional chemical methods are suitable for high degrees of water purification from dissolved oxygen. However, some of them (*e.g.*, reduction with hydrazine hydrate or sodium sulfite at elevated temperatures) have some drawbacks associated with the toxicity of used reagents (particularly, those based on hydrazine) or undesired presence of additional suspended solid particles in water (in the case of sodium sulfite).[1] The approach based on the use of metal nanoparticles proved to be the most promising and generally accepted modern method.[2 – 5]

In recent years, considerable progress in catalytic processes was achieved as a result of development of the concept put forward by V M Gryaznov[6 – 10] of catalytic membrane reactors, particularly, polymer catalytic membrane reactors.[11 – 14] The key idea was that a membrane serves as the catalyst and simultaneously provides the selective transfer of one component of the reaction mixture. For example, palladium membranes permeable only to hydrogen proved to be quite efficient in hydrogenation and dehydrogenation catalyzed by palladium. The removal of the dehydrogenization product (hydrogen) makes it possible to enhance the yield and selectivity of the equilibrium reaction, among other things, due to suppressing undesirable side processes. For liquid-phase hydrogenation, hydrogen is supplied on one side of the palladium membrane, selectively diffuses through the membrane and appears in its active form on the other side where hydrogenation occurs. It deserves mention that in the initial stage of these studies, relatively thick non-porous metallic membranes (foils and tubes 50 – 100 μm

thick) were used. For the practical use, the palladium layer thickness should be decreased.

The development of catalytic membranes based on metal/polymer composites is a radically new approach to the problem of reducing the consumption of expensive noble metals. In a relevant patent,[12] the polymer matrix was proposed to be made of polydimethylsiloxane with silica gel-immobilized palladium particles. Besides their low cost, such membranes display additional advantages. For example, for membranes with catalytic solid particles, the polymer matrix can be chosen in such a way as to exhibit different sorption capacity with respect to reactants and products, which would enhance the catalyst efficiency. The production processes of polymer membranes are well developed, so that their characteristics can be varied over broad limits; this is why organic polymers are now used in the fields that earlier employed only inorganic materials.[15–18]

The successful use of polymers is due to several factors. Among the major ones, mention should be made of the following aspect: a considerable number of catalytic reactions in fine organic synthesis are carried out in the temperature range from −20 to 200 °C and the majority of polymeric materials are sufficiently stable in this temperature range. Taking into account the versatility of polymer synthesis and the wide diversity of polymeric materials, one can find a polymer with properties to suit just a particular catalytic reaction. Moreover, it is not only the temperature stability of a material but also its resistance to acids, bases and various oxidants that is required. Methods of enhancing the stability of polymeric materials with respect to solvents have also been developed. The best known method consists of partial cross-linking of the polymer.

Ion-exchange materials (ion exchangers) are a kind of reactors.[2] For synthesizing metal/polymer composites by the chemical deposition of metals, the use of ion-exchange matrices containing charged sites may prove to be preferable because in this case, the amount of deposited metal and its distribution throughout the matrix can be controlled. The metal in an ion-exchange matrix can exist as fine particles (as a rule, nanoparticles) in the zero-valent state or as a part of oxides, poorly soluble hydroxides, simple or complexing salts fixed in the polymer matrix (Fig. 1). The matrix can exhibit cation- and anion-exchange or complexing behaviour. By immobilizing metals in polymer matrices, the catalytic and chemically active composite materials can be prepared in which two types of reaction sites coexist: the dispersed metal particles and the ionogenic matrix centres. In the presence of counter-ions located near the fixed charged groups, the metal/ion exchanger composites exhibit ionic conduction. The metal component and also the matrix with its conjugated bonds can promote electron conduction of the composite. The ion-exchange matrix stabilizes not only metal particles but also metal oxidation products. In view of the fact that metal/ion exchanger nanocomposites are simultaneously capable of electronic (redox) and ion-exchange reactions, they are referred to as electron ion exchangers and called redoxites.[19–22]

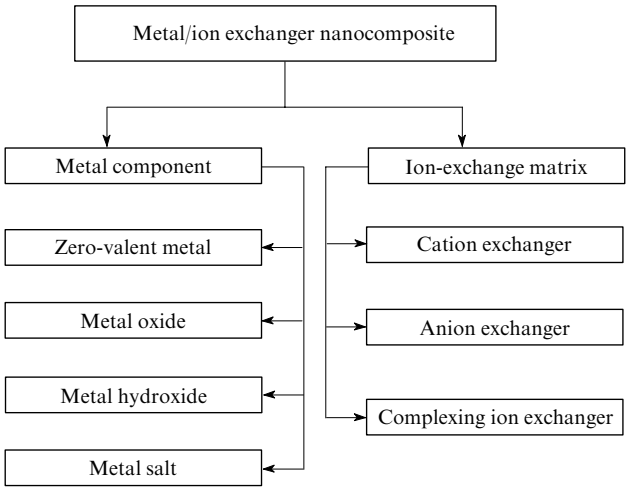


Figure 1. Components of a metal/ion exchanger nanocomposite.[2]

In the present review, we discuss the methods of synthesis of metal nanoparticles and metal/polymer nanocomposites, in particular, ion-exchange systems. Attention is concentrated on the membrane catalytic systems used in the advanced removal of dissolved oxygen from water. The most efficient systems that make it possible to reach record-breaking degrees of water purity with respect to oxygen are described. The review includes an analysis of a variety of processes — from the synthesis of nanoparticles to special methods of oxygen removal.

II. Synthesis of nanoparticles

The methods of synthesis of nanoparticles are widely diverse (for instance, see Refs 23–27). We will consider several main methods which serve as the basis for the development of their various versions aimed to control not only the size and composition but also the shape of nanoparticles. Note that nanoparticles are thermodynamically unstable systems. The use of nanoparticles in applied technologies brings about the problem of conservation of their functional properties and their stabilization. This problem should be solved in each particular case. The main methods that provide stability of nanoparticles are discussed below.

1. Method of evaporation–condensation

The procedure of evaporation–condensation forms one of the main methods of preparation of metal nanoparticles.[28] According to this method, the metal is evaporated into an inert gas flow, the gas with metal vapour is fed into a chamber with the wall temperature varying by a certain law. The temperature variations are usually calculated based on the heat and mass transfer equations and the kinetics of nucleation in order to provide the necessary rate of metal vapour condensation at which the particles have time to grow to the desired size.

The grown particles should be deposited on a substrate where they lose their mobility. The deposition should be quick because nanoscale particles are very mobile and due to their thermodynamic instability stick together to form sufficiently stable aggregates in which they easily coalesce. The detailed studies of the kinetics of nanoparticle aggregation during their synthesis by the evaporation–condensation method have shown[29] that, for example, nanosized zinc particles manage to aggregate in 10–100 ms depending on their growth mode. This produces a fractal structure with the logarithmically normal size distribution, where the average size of aggregates fits the micrometre region.

Nowadays, the interest in the evaporation–condensation technique pertains because it affords metal particles of the highest purity. The improvement of the method is largely associated with the search for approaches for depositing nanoparticles not onto a solid substrate but into the liquid phase, which opens up the possibility of further manipulation of nanoparticles. Methods were proposed [30, 31] in which the solid substrate was replaced by conventional solvents, co-deposition of the solvent and the particles took place and thus the volume of nanoparticle-involving composite could be gradually increased. By subsequent heating, the composite was transferred into a colloid dispersion of nanoparticles. By an analogous scheme, the metal/polymer nanocomposites can be synthesized [32, 33] provided that monomer polymerization is carried out after co-deposition of the monomer and nanoparticles. This scheme is implemented rather easily, for instance, with polyxylylene.

However, colloid dispersions prepared according to the above scheme are also not always stable. To overcome this problem, it was proposed [34] to add surfactants into the dispersion through their co-deposition (or subsequent introduction). As a result, solvent-dispersed nanoparticles measuring down to 1 nm with the concentration of up to 10^{20} particles per m^3 were synthesized. According to electron microscopic studies, no aggregates were formed in such systems.

The first experiments on the synthesis of colloid dispersions by the evaporation–condensation method were carried out with silver nanoparticles. Later, using this method, nanoparticles of Bi, Cu, Te were synthesized.[35] For all systems under study, it was shown that by varying the pressure and composition of the carrying gas, particles measuring from 1 to 10 nm can be formed. The particles had a sufficiently narrow size distribution: the standard deviation fitted the range from 1.4 to 1.6. Dimesso *et al.*[36] synthesized nanoparticles of Ag–M (M = Co, Fe, Ni) alloys with similar characteristics.

The method of evaporation–condensation has not found wide use for several reasons (although, as was mentioned above, it is most attractive from the standpoint of synthesizing pure nanoparticles). First of all, this method is characterized by low efficiency. Second, according to the modern concepts, the nanoparticle size dispersion is too wide. Third, fine variation of the size of nanoarticles requires considerable effort. The classical colloidal methods of nanoparticle synthesis are more popular. Their attractiveness has been revived due to the appearance of a wide class of surfactants that allow one to tune nanoparticle characteristics.

2. Method of reduction from solutions

Metal sols are conventionally synthesized by chemical reduction.[37] As the precursors, the corresponding metal salts and various reducing agents are used. To suppress the aggregation of particles formed, the reduction is carried out in the presence of stabilizing agents (special ligands, polymers, surfactants).[38, 39] The particle size cannot be predicted

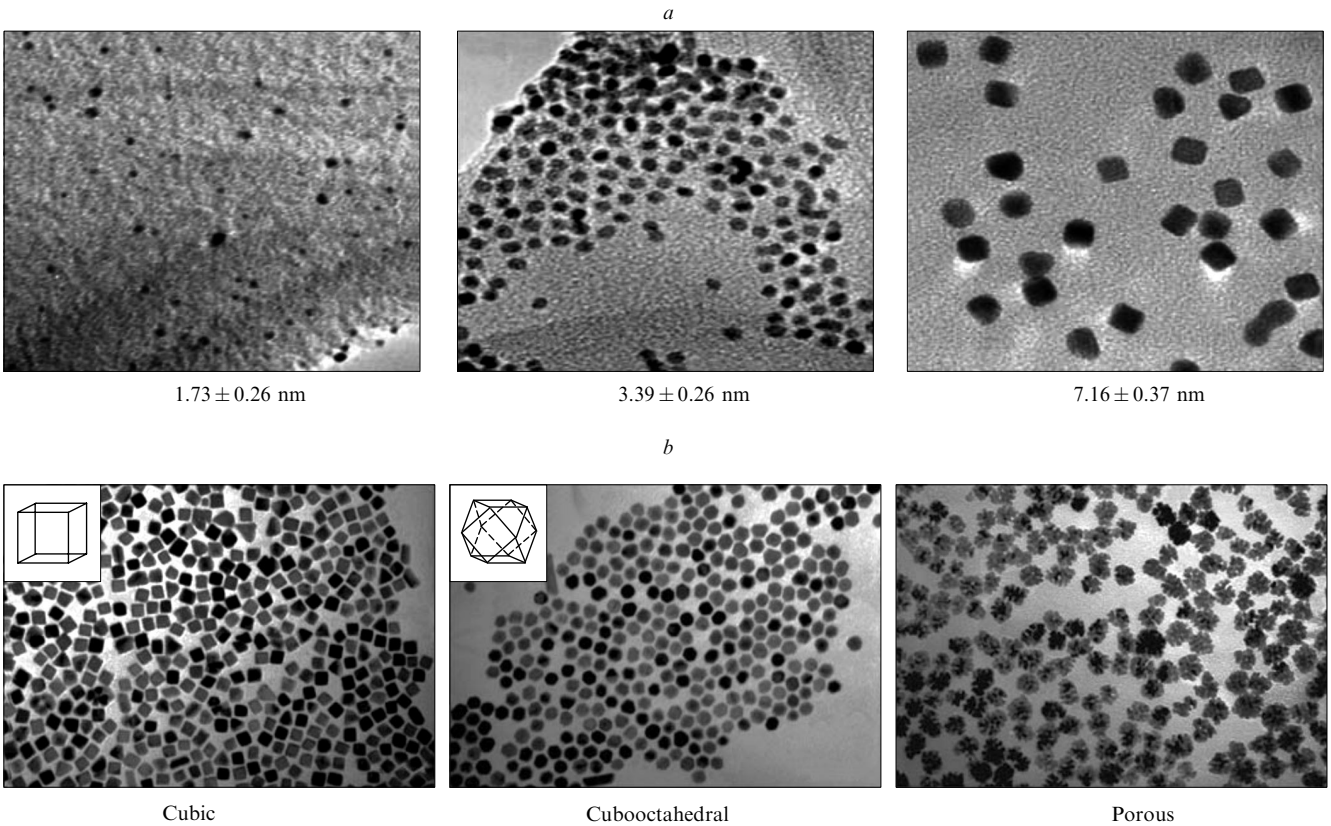


Figure 2. Illustration of the possibility of varying the size and shape of platinum nanoparticles prepared by chemical reduction method. (*a*) Particles of various sizes stabilized by polyvinylpyrrolidone,[43] (*b*) particles of various shapes stabilized by cetyltrimethylammonium bromide.[53, 54]

because it depends on several factors, namely, the nature of solvent and stabilizer and their concentration, the temperature and the reaction time.

It is well known [40, 41] that the attained supersaturation largely determines the particle size: the higher the supersaturation, the finer the resulting particles. By varying supersaturation, one can control the nanoparticle size.[42] Recently, for this purpose, the inhibitors of particle growth were brought into use, which play the dual role: on the one hand, they inhibit the removal of the reduced metal from solution thus increasing supersaturation and, on the other hand, they limit the particle growth rate. Usually, to inhibit the particle growth, the adsorbed layers (adlayers) of surfactants, polymers [43–49] or block copolymers [50–52] are used. Both the size and shape of nanoparticles can be controlled. Thus, it was shown [53, 54] that platinum particles can not only be shaped hexagonal or cubic but also can acquire the intermediate shape of cubooctahedra (Fig. 2). The surface of cubooctahedral particles is formed by (111) and (100) faces, whereas the surface of cubic particles is formed by only (100) faces. This difference is of principal importance for the catalysis.

Note that the nanoparticle shape is determined not only by synthetic conditions but also by the type of stabilizer used.[55] When metal is reduced in porous media, the particle size is obviously restricted by the pore size.[44, 56, 57] By using additional reagents, one can adjust the shape of synthesized nanoparticles. Roix *et al.*[58] used polyvinylpyrrolidone and silver salts as the additives in the synthesis of platinum nanoparticles in mesoporous silica gel. They have shown that regular nanoparticles (cubes, octahedra, cubooctahedra) can be prepared. Moreover, this synthesis can be carried in a different way to obtain platinum nanoparticles with finer silver nanoparticles deposited on their surface.

Note that sometimes nanoparticles fail to be deposited on the surface of certain oxides. Thus the gold deposition on the silica gel surface is impeded. This can be overcome by modifying the surface according to the sol–gel technology,[59] which is suitable for depositing thin layers on wide surfaces. For instance, the silicon dioxide surface can be coated with a thin layer of titanium dioxide, which rises the isoelectric point from 2 to 6, thus making easier the deposition of gold nanoparticles. This method can be used for the deposition of several modifying layers of different nature to obtain high-performance catalysts.[60]

Recently, not only traditional oxides (silica, alumina) but also carbon nanotubes [61–64] and oxide nanotubes [65] have been used as the porous media. In some cases, the use of nanotubes is associated with the necessity of modifying their surface to provide stronger binding of metal nanoparticles. Particularly, such modification is needed for producing efficient metal/carbon nanotube composites, which are used as proton-exchange membranes in fuel cells.[66] However, even fairly efficient modification of carbon nanotubes sometimes fails to suppress the aggregation of deposited metal nanoparticles, which are weakly bound to the tube surface.[67] According to one solution of this problem, the metal nanoparticle/carbon nanotube composite was coated by a silicon dioxide layer (<1 nm thick).[68–70] The oxide layer was deposited [70] onto carbon nanotubes containing a metal salt and the latter was then reduced in the hydrogen flow at high temperatures. In the presence of this protection layer, the catalyst stability substantially increased without any noticeable loss in its performance.

Some dendrimers, *i.e.*, polymers with a highly branched tree structure measuring 2–15 nm, can serve as the natural nanoreactors. Dendrimer molecules have hollows in which molecules and nanoparticles can be stabilized. After reduction, a nanoparticle is formed inside the dendrimer hollow (Fig. 3). Moreover, the dendrimer provides not only the hollow to house the formed nanoparticles but also the protective coating that prevents their aggregation. Dendrimers make it possible to efficiently regulate the size of nanoparticles at the level of 1 nm.[71–80]

The synthesis of silver nanoparticles measuring 7 nm by photochemical reduction in dendrimers with terminal amino and carboxyl groups occurs by the following scheme:[72]

$$Ag^+ + [dendrimer]—COO^- \xrightarrow{h\nu} Ag^0 + [dendrimer]—COO^{\bullet} \longrightarrow$$
$$\longrightarrow Ag^0 + [dendrimer]^{\bullet} + CO_2 \qquad (1a)$$

$$Ag^+ + [dendrimer]—NH_2 \xrightarrow{h\nu} Ag^0 + [dendrimer]—NH_2^+ \qquad (1b)$$

Synthesis of copper nanoparticles with the size of 2–4 nm stabilized by polyamide-imine was carried out.[71] The use of dendrimers containing thiol [73] or carboxyl [74] groups proved to be successful in the synthesis of gold nanoparticles, while the polyarylether-based dendrimers turned out to be a good choice in the synthesis of platinum

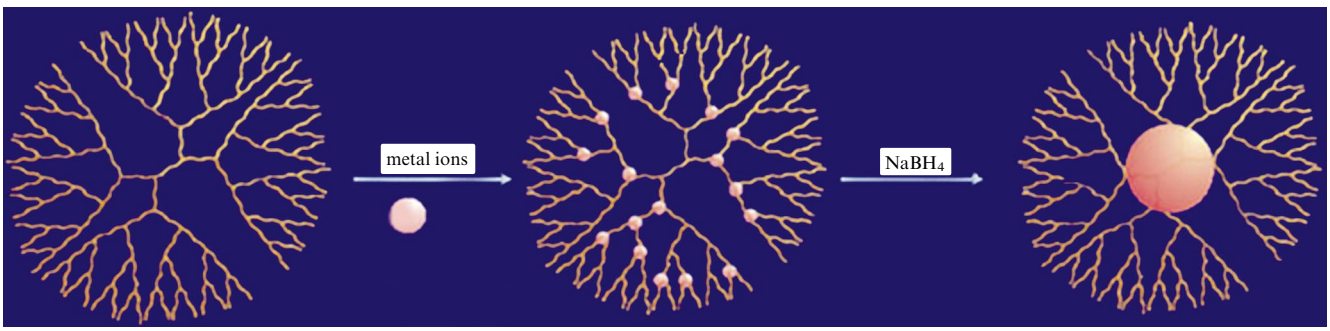


Figure 3. Illustration of the formation of a dendrimer nanocomposite.[78]

nanoparticles.[75] It is evident that dendrimers can also be used for synthesizing bimetallic nanoparticles.

Alkanethiols were successfully used as the stabilizing surfactant layers. Detailed studies[81–89] have shown that in the presence of alkanethiols, various procedures of gold reduction from $HAuCl_4$ solutions under the action of $NaBH_4$ produced virtually monodisperse particles. The resulting gold nanocrystals consisted of a metal core involving from 10 to 5000 atoms and a dense alkanethiol shell. Apparently, the efficiency of alkanethiols as the terminators of nanoparticle growth is determined by their ability to form dense self-assembled layers on the surface of gold single crystals.[90] The use of alkanethiols proved to be successful in the synthesis of silver nanoparticles.[90–96] Probably, alkanethiols could form self-assembled layers on the surface of other nanoparticles too.

Electron microscopic data have shown that gold single crystals are compact and have a face-centred cubic lattice.[87] The particles are predominantly shaped as octahedra or icosahedra. The nanocrystal size depends on the alkyl chain length and the thiol-to-gold ratio in the solution.[87,97] Single crystals consist of pure gold, while sulfur atoms are located only on the surface being bound to alkyl chains. The state of alkanethiol adlayers depends on the size of the metal core.[98] The alkyl chain has a more ordered conformation on coarser particles. The critical size is 4.4 nm. For larger particles, alkanethiol forms a two-dimensional layer, whereas on finer particles the adsorbed layer shows elements of the three-dimensional packing.

The ligand shell plays the important role in the structuring processes when nanoparticles are being distributed in the matrix. In connection with this, studying the behaviour of the ligand shell under different conditions is of fundamental importance. The restructuring of the ligand shell can occur upon replacement of the solvent in the colloid dispersion, deposition of nanoparticles on a substrate or incorporation of nanoparticles into the polymer matrix. Bauer *et al.*[99] studied in detail the structural transitions in alkanethiol ligand shells deposited on silver nanoparticles. They have shown that the restructuring processes in adlayers are determined by the nanoparticle size, the hydrocarbon fragment length and the dispersion medium. Correlations that can be used to control of the behaviour of nanoparticles under various conditions were established.

3. Combined nanoparticles

Recently, specialists in the field of catalysis focused attention on particles formed by several metals. In these particles, one of components is preferentially distributed over the surface of other components.[100] By using these systems, it is possible to tune rather finely the catalyst properties. Bimetallic catalysts are synthesized based on preliminarily obtained nanoparticles, which serve as the nuclei for deposition of the second metal.[101,102] For instance, in the synthesis of palladium/cobalt nanoparticles, palladium nanoparticles served as nuclei.[103] Nanoparticles iron/platinum, cobalt/platinum[104,105] and gold/palladium, gold/platinum[106,107] were also formed by this method. The metal layer on the nucleus surface may exhibit structural characteristics different from those of the compact metal, which considerably enhances the catalytic activity of nanoparticles.

The shells can be formed by nanoparticles on the oxide surface and also by oxides (or other inorganic substances) on the surface of metal nanoparticles.[24,108–110] A lot of metal core/oxide shell nanoparticles were synthesized with cores of transition metals (Pt, Pd, Ru, Ni, Co, Fe, Au, Cu) and oxide shells (ZnO, MnO_2, TiO_2, Fe_3O_4). The interest in these systems was associated with the fact that the metal/oxide transition area exhibits enhanced catalytic activity.[111,112] The difficulties in the development of such systems are mainly associated with the short time of shell formation, which complicates the reliable control over its thickness. There are wide prospects for the synthesis of oxide spheres with the size of $\sim$100 nm coated by metal nanoparticles. Methods have been developed for the formation of spherical particles of oxides of aluminium, cerium, titanium and zirconium[113] and also of mixed oxides such as lead niobate.[114] These systems are interesting as regards studying the catalytic processes,[115–118] because, on the one hand, they serve as well-characterized models and, on the other hand, they largely resemble real catalysts in their properties. The methods of synthesis of such systems were briefly surveyed.[110]

For example, consider the synthesis of silver and platinum nanoparticles on the surface of polystyrene spheres.[119] Here, a metal salt and organic monomers [styrene and a macromonomer, namely, poly-(*N*-isopropylacrylamide)] were added simultaneously to the solution, then co-polymerization in the presence of an initiator was carried out together with the reduction of copolymer-coordinated metal ions so that the resulting metal was distributed over the surface of polystyrene spheres.

Other methods of particle deposition are possible. Thus, nanoparticles can be coated by polyelectrolyte that bears a charge opposite to the charge of dielectric spheres, which results in heterocoagulation. Nanoparticles can also be bound by special groups grafted to the surface of oxide spheres. Moreover, the active sites on the surface of dielectric spheres can be used as nucleation centres for the reduced metal.[120]

Yet another method of formation of nanoparticles with unusual structure is based on the Kirkendall effect. This effect is associated with the difference in diffusion coefficients of components of the system (*e.g.*, binary). If one component diffuses faster than the other, excessive voids are left in the alloy. This may result in restructuring of atomic planes, as can be observed by migration of inert markers. Hollow nanoparticles may serve as a sort of nanoreactors. Such systems can be obtained most easily for nanoparticles or thin layers of cobalt, where cobalt sulfonation or oxidation reactions occur on the surface.[121] Cobalt atoms diffuse faster towards the shell surface than sulfur or oxygen atoms diffuse towards the metal core. As a result, voids are formed in nanoparticles. Thus the hollow nanoparticles of the 'nut' type with the metal core can be prepared (Fig. 4).

Hollow particles with metal cores are obtained in three stages.[121] First, a nanoparticle, *e.g.*, of platinum, is grown; then, a cobalt shell is formed thereon and then oxidized to form a void in which the platinum nanoparticle remains. The formation of voids was observed for Co/Co_9S_8, Co/CoO, Pt/CoO, Ag/Au and Fe/Fe_xO_y systems. Particles inside the void retain their catalytic activity. This is explained by the fact that, as a rule, the shell is polycrystalline and contains small pores through which reagents can penetrate into the void. Although the shell may decrease the rate of the catalytic process, it also plays an important role of preventing the aggregation and sintering of metal nano-

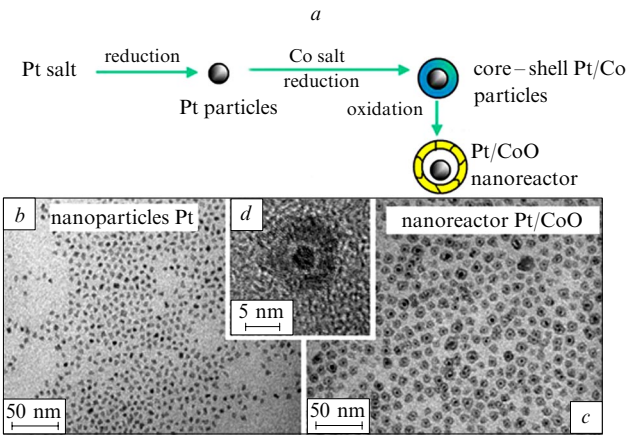


Figure 4. Schematic of preparation of nanoreactors (*a*) and images of original platinum nanoparticles (*b*, *c*) and nut-type nanostructures synthesized based on these particles (*d*).[121]

particles. Yet another advantage of the shell is associated with its low permeability, because small pores prevent the penetration of large molecules. The latter can enhance the selectivity of the catalytic process. Thus nut-type nanoparticles represent a catalytic membrane reactor in which the metal core serves as the catalyst and the porous shell operates as a selective inorganic membrane.

4. The effect of nanoparticle size and shape on their properties

It is a well known fact that the transition to nanosized particles is associated with a dramatic change in their catalytic activity.[24] The brightest example is the catalytic activity of gold nanoparticles.[122–128] The catalytic properties of gold nanoparticles with respect to carbon monoxide oxidation were surveyed and numerous experimental and theoretical data were analyzed in a review.[129] The possibility of commercial use of gold-based catalysts was discussed.[130] At the same time, it deserves mention that there is no direct correlation between the catalytic activity of nanoparticles and their size. A lot of publications were devoted to detailed investigation of this correlation; these studies are generalized in Refs 55 and 131.

As the nanoparticle size decreases, the nanoparticle specific surface area increases; however, the reaction rate per unit weight of the catalyst does not necessarily increase.[132–137] Thus, in the hydrogenation of 2,4-dinitrotoluene to form 2,4-diaminotoluene, the coarse palladium nanoparticles exhibit high catalytic activity because the particle activity in hydrogenation is determined by the formation of the palladium hydride surface phase, which occurs more readily on coarse particles.[132] In contrast, for reactions involving NO and CO to produce mainly N_2 and CO_2, the catalytic activity increases with a decrease in the nanoparticle size, but not in the direct proportion to the increase in the nanoparticle surface. This is explained by the increase in the fraction of the surface area coated by strongly bound nitrogen, resulting in a decrease in the number of sites for NO dissociation.[137]

The catalytic activity of particles is determined to a large extent by their shape. The catalytic activity of palladium nanoparticles in the Suzuki reaction between phenylboronic acid and iodobenzene was studied.[138] In experiments, the nanoparticles measuring 3.0, 3.9, 5.2 and 6.6 nm were examined. Their catalytic activity was determined from the reaction turnover frequency *vs.* the number of surface atoms. The turnover frequency decreased in the following sequence of nanoparticle size: 3.9 > 3.0 > 5.2 > 6.6 nm. The calculation of the catalytic activity for the number of atoms located on vertices and edges of polyhedral nanoparticles revealed no relationship between the turnover frequency and nanoparticle size. This confirmed once again the generally accepted opinion that the edges and vertices of such nanoparticles serve as the active sites of these catalysts.

The concept of active sites on the catalyst surface was put forward rather long ago.[100] The rate of each catalytic reaction depends on its own active sites, which determine the height of the energy barrier to the rupture of a particular bond. For example, in hydrocarbon reactions, the C–H bond cleavage on platinum surface steps proceeds more easily than the break of a C–C bond.[139] On kinks, in contrast, C–C bonds are broken more easily. The effect of the catalytic site structure on the reaction parameters was surveyed[140] and for CO oxidation, the relationship between the reactivity and the electronic structure of active sites was examined. In this case, the selectivity of the catalytic reaction is determined by the ratio of concentrations of active sites of different natures. This ratio can be varied by adjusting the size and the shape of nanoparticles. However, it deserves mention that the ratio of concentrations can also change in the course of the reaction.[139]

Narayanan and El-Sayed[141,142] studied how the particle characteristics change in different reactions. In particular, they have shown[141] that during the Suzuki reaction, the palladium nanoparticles stabilized by polyvinylpyrrolidone become coarser due to the Ostwald ripening of the dispersion. When the reaction was carried out for a long time, even sedimentation of particle aggregates was observed as well as the transformation of tetrahedral nanoparticles to spheres.[142]

Thus, the preset size and shape of synthesized nanoparticles can change during operation of a catalytic reactor. Recently, the interest in atomic-level studies into changes of nanoparticle properties during catalyst operation has increased. Due to application of new devices and miniaturization of reactors, considerable progress was achieved in investigation of the particle properties and their changes under conditions resembling the real conditions of industrial processes. To determine the structural characteristics of catalyst nanoparticles during their work, the following methods were used: scanning transmission microscopy, high-pressure scanning tunnelling microscopy, sum frequency generation spectroscopy, X-ray electron spectroscopy at atmospheric pressure, diffuse reflectance IR spectroscopy, surface-enhanced Raman spectroscopy, environmental transmission electron microscopy, analysis of the electron energy loss near-edge fine structure, quartz crystal microbalance, X-ray diffraction, small-angle/wide-angle X-ray scattering, thermogravimetric analysis, near-edge X-ray absorption fine structure spectroscopy (NEXAFS), extended X-ray absorption fine structure spectroscopy (EXAFS), quick-scanning EXAFS, field ion appearance energy spectroscopy. The data on the potentials and the practical use of the listed methods can be found in several publications.[131,139,143–151] Note that theoretical modelling also considerably helps to interpret experimental data.[151]

5. Deposition of particles on supports

As was noted above, the progress achieved in the synthesis of nanoparticles made it possible to control not only their size, but also their shape so that the attention was shifted from well characterized planar surfaces of single crystals to catalytic properties of nanoparticles.[152] Well-characterized surfaces are convenient study objects; however, they fail to reflect many specific properties of catalysts, for instance, their turnover frequency and selectivity, because these characteristics are predominantly determined by the presence of steps, kinks and other surface defects. The important factor determining the catalyst properties is the interaction of nanoparticles with the support; hence, the relationship between the catalytic activity and the nanoparticle distribution over the support was studied.

A method that can be used to control the nanoparticle distribution on the surface is associated with the use of Langmuir troughs.[153] A monolayer of hydrophobized nanoparticles is placed on the surface (*e.g.*, of water). By varying the pressure in the monolayer, it is possible to create in it a certain density of nanoparticles which is retained after the monolayer has been transferred to the support. Figure 5 shows the structure of monolayers of platinum nanoparticles, which were formed at different pressures within the monolayer. By depositing several monolayers, it is possible to form not only two-dimensional but also three-dimensional assemblies of nanoparticles.

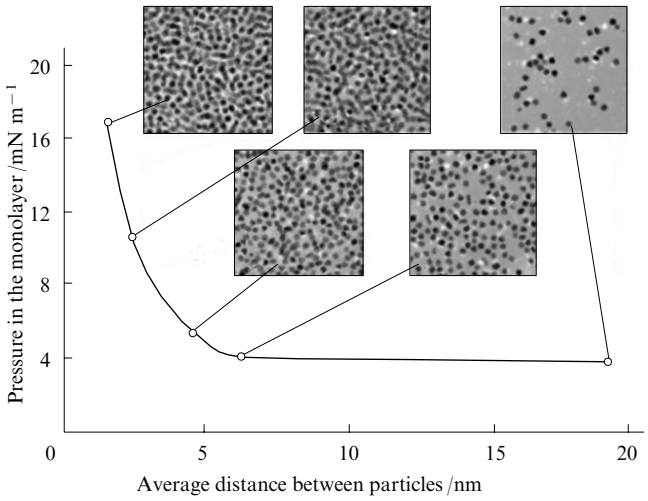


Figure 5. Dependence of the pressure in the monolayer on the average distance between nanoparticles and microscopic images of nanoparticles.[152]
Image size 100 nm.

Another efficient method for nanoparticle ordering on the surface is electron-beam lithography (*e.g.*, see Ref. 154). This method makes it possible to form catalytic systems of various metals deposited on different supports. The resulting catalysts not only can be adequately characterized for carrying out model reactions but also make it possible to follow the changes in the catalyst parameters during reactions.

Layers of catalytic particles were grown directly on the membrane surface to be used later for oxygen removal.[4] It was shown that such layers can be deposited on membrane modules (for details, see below).

III. Catalytic polymer membranes

All the aforementioned methods are engaged in the synthesis of metal/polymer nanocomposites used as catalytic materials for membranes. Each method has its own special features, which should be taken into account. Thus, the use of a scheme according to which the catalyst is formed simultaneously with the membrane brings about additional complications associated with the possible effect of strong polymer–catalyst interactions.[15] This group of methods includes the membrane synthesis by the phase inversion process in which a porous polymer matrix is deposited from solution upon temperature variations or solvent replacement and the particles that usually serve as the new phase nucleation centres may have a strong effect on the morphology of the polymer membrane formed (moreover, this effect can also be very strong even at the low catalyst content). An important condition of this method is that stable dispersions of catalyst particles in the polymer solution should be formed in the first stage. Otherwise, the synthesized membrane can turn out to be strongly inhomogeneous as regards both its structure and the catalyst content. It is necessary for the catalyst to retain its activity during the membrane formation.

The uniform distribution of particles throughout the membrane can be promoted by the polymer itself; this is why catalytic membranes are often prepared using branched macromolecules or block copolymers in which micellar structures can be formed and can serve as microreactors in the synthesis of nanoparticles preventing their aggregation and sintering. These can also be polymers cross-linked either physically or chemically and containing incorporated particles.[155] Sometimes nanoparticles coated by a stabilizing polymer layer are grafted on a cross-linked polymer matrix to obtain a sufficiently stable supported catalyst.[156]

To provide the uniform distribution of particles throughout the polymer matrix, special techniques were emplyed. For instance, in the synthesis of catalytic membranes, solutions of pre-polymers and cross-linking agents were used (Fig. 6). The solvent favours a uniform distribution of particles throughout the polymer matrix; however, this gives rise to other problems, because particles can sediment from the solution, and this also contributes to the non-uniform distribution. The sedimentation can be suppressed as follows:[157] the polymer is initially partly cross-linked by rising the system temperature and the resulting sparse network prevents sedimentation of catalyst particles.

The catalyst-containing polymer membranes are rather often obtained by the reduction of the metal from its precursor originally dissolved together with the polymer, either before or after the preparation of membrane films. To date, a lot of information has been accumulated on this method, which is described in detail in the literature.[16] For hydrogenation in gas and liquid phases, both porous and non-porous polymer catalytic membranes with palladium particles as the catalyst were used.[5]

To characterize the state and properties of nanoparticles in polymer matrices, the following methods were used: IR and Raman spectroscopies,[158] X-ray photoelectron spectroscopy,[159] electron microscopic techniques (scanning, trans-

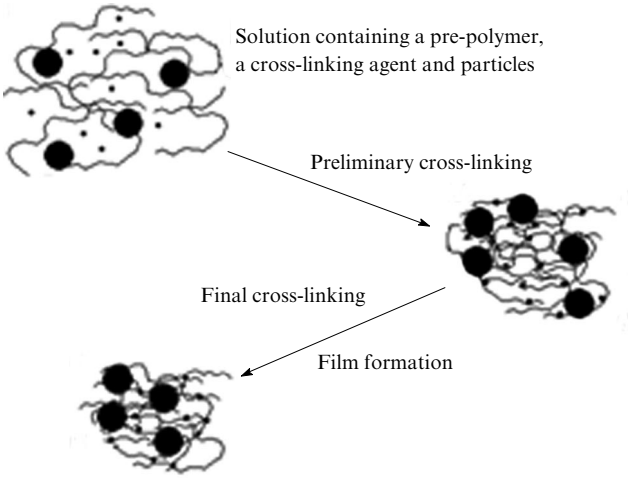


Figure 6. Formation of a catalytic membrane with the preliminarily partially cross-linked polymer.

mission, atomic force and ion field methods),[158] nuclear magnetic and electron paramagnetic resonance spectroscopy, thermogravimetry, *etc*. The modern experimental physicochemical methods make it possible to follow the evolution of nanoparticles during their formation from precursors.[160]

In recent years, a trend has been emerging towards the development of unique methods for the synthesis of polymer membranes with incorporated catalyst nanoparticles. Among the wide diversity of original methods, the following should be mentioned: the layer-by-layer adsorption of polyelectrolyte and nanoparticles,[161,162] the synthesis of nanoparticles by employing specific polymers,[159,163] the modification of the inner surface of ultrafiltration membranes with oxides,[164] the electrospraying (electroforming) of solutions containing a polymer and a nanoparticle precursor.[165] A convenient synthesis of nanocomposites is by the ligand exchange reaction. For example, palladium nanoparticles in polyaniline were synthesized in this way.[160] Polymer catalytic membranes can be prepared by irradiating the nanocomposite precursors with electromagnetic[166] and supersonic[167] waves. In certain cases, the catalytic membrane composite material is first prepared from a polymer and a precursor of cluster-type nanoparticles[167–170] and only after this, the proper nanoparticles are synthesized.

IV. Nanocomposites based on ion-exchange materials

Among nanocomposites, an important place belongs to ion-exchange materials including polymer ion exchangers.[2] In the design of these nanocomposites, certain specific factors should be taken into account, particularly, the fact that the method of metal insertion into the ion-exchange matrix depends on the nature of the matrix.

Ion-exchange polymers contain pores of various type and size, capable of serving as both reactors for the synthesis and transport channels. Depending on the size, three types of pores are distinguished: micropores (0.3–2 nm), mesopores or middle-size pores (2–50 nm) and macropores (>50 nm). Pores can be either closed (isolated from one another and having no exit to the surface) or through (shaped as channels connected with one another and with the surface). We will consider particular systems.

1. Cation-exchange systems

In the chemical deposition of a metal into a cation-exchange matrix (cation exchanger), an aqueous solution of a usual or complex metal salt is used as the saturation solution. This solution reacts with the cation exchanger in its H^+-form according to the ion exchange saturation reaction

$$z\,RSO_3^-H^+ + MX_z \longrightarrow (RSO_3^-)_zM^{z+} + z\,HX \qquad (2)$$

and the metal ions arriving to the ion exchanger are concentrated near the ion-exchange groups as the counter-ions. The number of cations incorporated during the time required for complete saturation of the ion exchanger is equal to the total exchange capacity. Then, the cation exchanger is treated with a solution of alkali (sodium hydroxide) to induce the formation of a poorly soluble compound in polymer pores near the ionogenic groups. The following ionic reaction of deposition proceeds:

$$(RSO_3^-)_zM^{z+} + z\,NaOH \longrightarrow [RSO_3^-Na^+]_zM(OH)_z \qquad (3)$$

The synthesis of hydroxide-containing composites is completed at this point.

The composites containing zero-valent metal are synthesized by the redox reaction of metal deposition from its hydroxide precursor (Red is the reducing agent, Ox is the oxidant):

$$[RSO_3^-Na^+]_zM(OH)_z + Red \longrightarrow [RSO_3^-Na^+]_zM^0 + Ox \qquad (4)$$

or directly from the precursor of the metal counter-ion. The process is completed with an ion-exchange reaction that transforms the ion exchanger into its initial ionic form

$$[RSO_3^-Na^+]_zM^0 + z\,HX \longrightarrow [RSO_3^-H^+]_zM^0 + z\,NaX \qquad (5)$$

Repetition of the reaction cycle (2)–(5) produces the $[RSO_3^-H^+]_zM_n^0$ material with the preset capacity with respect to metal. Here, n is the number of metal atoms per z moles of the ion exchanger.

Metal deposition may often involve processes the result of which depends on penetration of co-ions rather than counter-ions into the ion exchanger. For cation-exchange membranes, this is true for all reducing agents of the anionic type (dithionite, borohydride and other anions). Conversely, in anion-exchange systems, metal ions function as co-ions.

2. Anion-exchange systems

Treating an anion exchanger in its initial OH^- form with a metal salt solution makes it possible to immediately precipitate the metal as a poorly soluble compound in the vicinity of ionogenic groups; then the redox reaction of metal deposition with simultaneous recovery of the original ionic form of the ion exchanger can be carried out, for instance,

$$z\,RNMe_3^+OH^- + MX_z \longrightarrow [RNMe_3^+X^-]_zM(OH)_z \qquad (6)$$

$$[RNMe_3^+X^-]_zM(OH)_z + Red, NaOH \longrightarrow \qquad (7)$$

$$\longrightarrow [RNMe_3^+X^-]_zM^0 + Ox$$

First, the ion-exchanger ionogenic groups can be saturated with anions of the reducing agent and then the metal co-ions are reduced.

As mentioned above, the nature and concentration of all components of the system affect the size of chemically deposited metal particles. Hence, the signs of charges of the reducing agent (cation, anion or neutral molecule) and the polymer matrix and also the presence of a complexing agent in solution will determine the size of metal particles obtained upon chemical deposition into polymer matrices.[171–173] The nature of anions in metal salts was found to affect the resulting particles.[174]

Thus by selecting the ion-exchange matrix, the reducing agent and the complexing agent, it is possible to prepare the metal/ion-exchanger composites with different size of metal particles.

Nanocomposites containing matrix-immobilized metals chemically reactive with respect to oxygen were first synthesized back in 1949[175] from anion exchangers by treating them with solutions of copper and silver salts followed by the reduction of ions of these metals with sodium dithionite. It was proposed[21] to combine the ionogenic and redox functions in a single cation exchanger. The metal-containing nanocomposites were prepared based on sulfo and carboxyl cation exchangers that existed either as gels or in the condensed state; the highest reducing capacity was typical of copper and bismuth-containing nanocomposites based on sulfonated shale oil cake. The electron-exchange properties of such activated carbons were due not only to the metal but also to their intrinsic quinoid groups.[176, 177] Besides zero-valent metals, transition metal hydroxides (iron, nickel, copper, manganese) in low oxidation states are often deposited into ion exchangers.[178–181]

Nanocomposites that combine the reducing properties of polymers and metals have been synthesized. Treating polymers containing hydroquinone or pyrrogallol with copper salts with the subsequent reduction of the salts produced electron-ion exchangers the reducing properties of which were determined by redox groups of the matrix and copper particles in the matrix pores (see Ref. 182, p. 147). Based on macroporous ion exchangers, a high performance copper/hydrazine nanocomposite that contained copper complexes with hydrazine and metallic copper has been prepared.[183]

By immobilizing metal nanoparticles (palladium, iron, nickel, indium) in ion-exchange zeolite matrices, materials chemically reactive with respect to irreversible oxygen sorption from gases can be synthesized.[184]

Nanocomposites were also prepared in the form of metal-containing fibres.[185] The chemical or electrochemical reduction of metal to its zero-valent state took place throughout the mass of a fibrous ion-exchanger so that the metal did not mechanically shed. Thus, a palladium-containing composite was prepared based on sulfo cation exchange fibres.[186] The main advantage of metal-containing fibres is the high rate of reactions.

Yet another method is associated with modification of ion-exchange membranes. By introduction of metals such as Pd, Ni, Ru, Rh, Au, Ag into ion-exchange membranes Nafion, MF-4SK and also into polyaniline (PANI) membranes, the catalytically and chemically active materials of a new type can be obtained.[187–190] Particularly, silver and silver sulfide nanoparticles were synthesized in nanopores of a perfluorinated ion-exchange membrane.[191]

Three-dimensional polymer chains form the basis of the spatial structure of metal/ion exchanger nanocomposites. As a whole, such nanocomposites represent highly porous swelling materials that consist of a polymer framework, fixed ions, counter-ions and metal particles (Fig. 7).

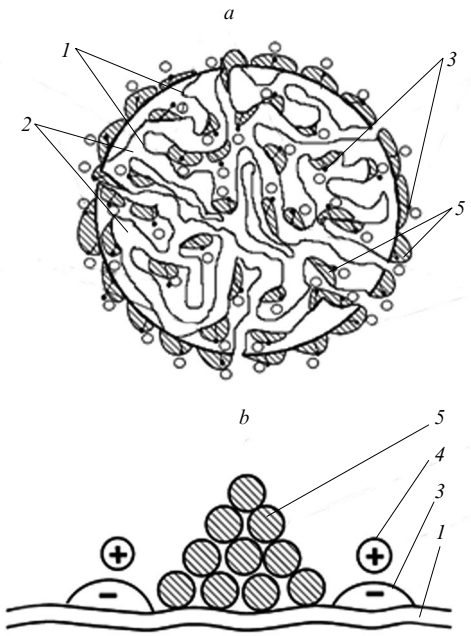


Figure 7. Schematic of a grain (*a*) and a pore fragment (*b*) for metal/sulfo cation exchanger nanocomposite.[2]
(*1*) Polymer chain, (*2*) pore, (*3*) fixed (SO_3^-) group, (*4*) counter-ion (H^+), (*5*) metal site (M^0).

The macroscopic structures with pores of 50–100 nm should be preferred. In macropores, metal particles occupy individual regions in the vicinity of ion-exchange groups (Fig. 8). According to microscopic examinations, their size varies from 5 to 500 nm. The distribution of metal throughout the ion-exchanger volume is relatively uniform. The macroporous structure provides sufficient diffusion permeability. The metal occupies from 3%–4% to 16%–25% of the pore volume. As a result, ionogenic groups are only slightly shielded by the metal and the oxygen diffusion coefficients determined from kinetic data are sufficiently high. In low-capacity composites, for example, copper-containing composites (with metal concentration of 0.8–1.0 mg-equiv cm^{-3}) based on macroporous sulfo cation exchanger KU-23, the metal particles are located at a distance of no less than 100 nm from one another. For the copper content of up to 10 mg-equiv cm^{-3}, no substantial change in the particle size was observed.

X-Ray diffraction analysis of samples with different copper contents has shown that the metal particle size was 33–50 nm irrespective of the number of deposition cycles (Table 1).

To obtain electrocatalysts, the metal was deposited into ion-exchange polymer films applied on electrode materials.[192] The formation of metal particles starts from the support and their further growth proceeds from particle to particle with the retention of contact between them. The use of ion-exchange polymer materials in the form of films gives

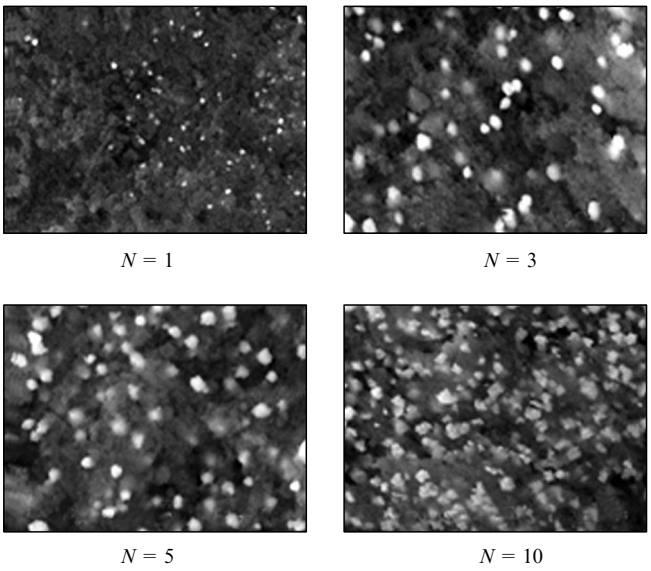


Figure 8. Microscopic images of a cross-section of copper/sulfo cation exchanger KU-23 nanocomposite.[2]
N is the number of saturation–reduction cycles; $Na_2S_2O_4$ as the reducing agent; magnification 10^4.

Table 1. Size of copper particles (d) as a function of copper content in a sulfo cation exchanger KU-23 according to X-ray deffraction analysis results ($Na_2S_2O_4$ as the reducing agent).[2]

Cycle No.	Capacity for copper / mg-equiv cm^{-3}	Diffraction peak half-width, 2θ /deg	Diffraction peak maximum position, 2θ /deg	d / nm
1	0.94	0.38	43.3	41
2	–	0.41	43.3	33
3	2.98	0.37	43.3	38
4	–	0.36	43.3	42
5	4.82	0.34	43.3	45
6	–	0.34	43.3	44
7	6.96	0.32	43.3	50
8	–	0.33	43.3	48
9	–	0.35	43.4	41
10	9.50	0.35	43.3	42

ultradisperse metal deposits with the grain diameter of 3–5 nm and the high specific surface area.

V. Membrane methods of oxygen reduction

In the present review, we mainly consider the problems related to the use of nanocomposites for the removal of dissolved oxygen from water.

An efficient method of advanced water purification from dissolved oxygen consists of its reduction by hydrogen on a palladium catalyst.[193–198] In their experiments, Huang *et al.*[194] used Pd-containing microparticles of individual polyaniline or polypyrrole (PPR) and also modified with SiO_2 (PANI–SiO_2 and PPR–SiO_2, respectively). Hydrogen was bubbled through 500 ml of deionized water with distributed Pd-containing microparticles (50 mg). The best results were obtained for catalysts based on the completely reduced PANI form (leucoemeraldine) with the addition of SiO_2 (LM–SiO_2 sample). The concentration of dissolved oxygen decreased from 860 to <100 μg kg^{-1} for LM–SiO_2 microparticles with the palladium content of 0.01 mass %.

It should be noted that the catalytic removal of dissolved oxygen from water is a vivid example of the commercial use of palladium catalyst deposited on an ion-exchange resin.[199,200] The process includes two stages: the dissolution of hydrogen in water and feeding water to the catalytic reactor.

A patent has been granted[201] on the method of deposition of metallic palladium on the external surface of polymer membranes. This disclosure was used to develop a single-stage method for the removal of dissolved oxygen from water in a catalytic membrane reactor with the use of Pd-containing polypropylene hollow-fibre porous membranes (Fig. 9).[4,5,202–206] Water that contains dissolved

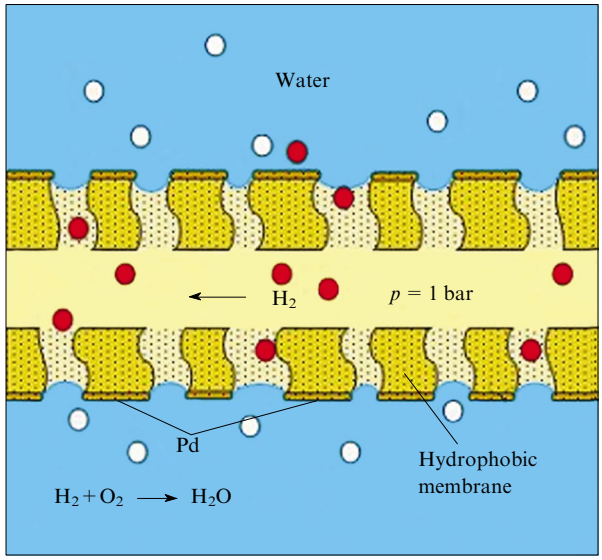


Figure 9. Schematic of oxygen removal from water with the use of porous hollow-fibre catalytic membranes.[206]

oxygen surrounds the external surface of a hydrophobic hollow-fibre membrane, while hydrogen is fed to hollow fibres and migrates through the membrane pores to the Pd-containing surface where the heterogeneous catalytic reaction of oxygen reduction by hydrogen to form water takes place. The hydrophobic porous catalytic membrane should perform three main functions, namely, it provides

— the distinct and easily controlled position of the gas/liquid interface;

— the accessibility of catalyst for reactants (hydrogen and oxygen);

— high hydrogen mass transfer parameters.

Palladium was deposited on the external surface of polymer membranes in the course of reduction of its salts by methanol, which served as both the reducing agent and the solvent. To enhance the adhesion of metal particles to the polymer, the membrane surface was preliminarily treated with organic solvents and a mixture of inorganic acids or with alkali solutions.

The discussed method was also implemented for the deposition of palladium on polypropylene membranes

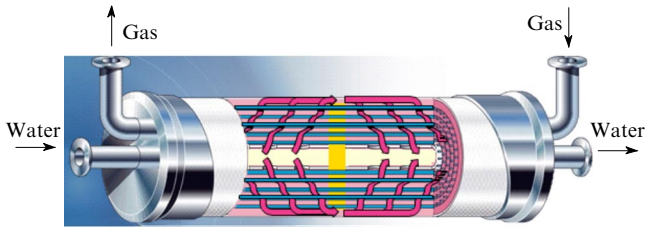


Figure 10. Membrane contactor.[193]

located inside an industrial membrane contactor (Fig. 10) without its disassembling. The structure and morphology of palladium nanoparticles on the membrane surface were studied by X-ray diffraction analysis, extended X-ray adsorption fine structure spectroscopy (EXAFS), scanning electron microscopy (including energy-dispersive analysis) and optical microscopy.

Interesting results on the structure and catalytic properties of palladium adlayers on the surface of polypropylene membranes were reported.[4] Two modes, stepwise and continuous, were used for palladium deposition (the resulting membranes are designated below as MC-S and MC-C, respectively). The samples of the MC-S series were synthesized by varying the time of palladium deposition onto the external surface of membranes, which took several tens of hours. The palladium salt solution in methanol was renewed every five hours. In the continuous mode, palladium was deposited also for several tens of hours but without replacement of the palladium salt solution in methanol. Figure 11 shows the microscopic images of membranes with deposited palladium.

A computer-assisted analysis of images presented in Fig. 11 has shown that the membrane surface porosity increases after the pretreatment. The porosity was $12 \pm 1\%$, $17 \pm 2\%$ and $17 \pm 3\%$, respectively, for the original, pretreated and palladium-containing membranes. The membranes retained their hydrophobicity after the palladium deposition.

In the X-ray diffraction analysis, the coherent scattering region (CSR) of the X-ray wave was chosen as the parameter characterizing the structure of palladium associates on the membrane surface. The CSR was found to be ~ 40 nm for MC-C catalytic membranes and ~ 10 nm for MC-S membranes (synthesized by the stepwise procedure). According to SEM data, the associates of palladium clusters mainly contained isolated clusters and their aggregates, their sizes varying in the ranges from 10 to 500 nm and from 200 nm to several tens of micrometres, respectively.

The kinetics of oxygen removal at different water flow rates is illustrated by dependences shown in Fig. 12. It is evident that the increase in the flow rate (u) induces a sharp increase in the rate constant for this process (according to estimates, as u^n, where $n \approx 1$). Hence, the rate of this process is limited by the oxygen transfer from the water bulk to the membrane surface. Insofar as in various flow modes, the transfer rate is usually proportional to the volume concentration of oxygen, the oxygen removal process is a first-order reaction. The strong dependence of the transfer rate on the hydrodynamic mode suggests that the near-surface flow is not entirely laminar. Apparently, the roughness and the irregular shape of the membrane surface induce weak turbulization of the near-surface flow. In the presence of the turbulent layer formed at a rough surface, the substance transfer rate is proportional to its volume concentration and the flow rate. Hence, the kinetics observed in the reactor approximately corresponds to a weak turbulent mode of oxygen transfer to the surface.

The first reaction order was confirmed[4] by measuring the rate of oxygen removal as a function of its current concentration in water. Figure 13 shows the data obtained for membranes modified in the continuous and stepwise modes. In both modes, the amount of palladium was 34 μg cm^{-2}. The rate of removal of dissolved oxygen from water was determined by the formula

$$w = \frac{c_{i+1} - c_i}{(t_{i+1} - t_i) S_m} \qquad (8)$$

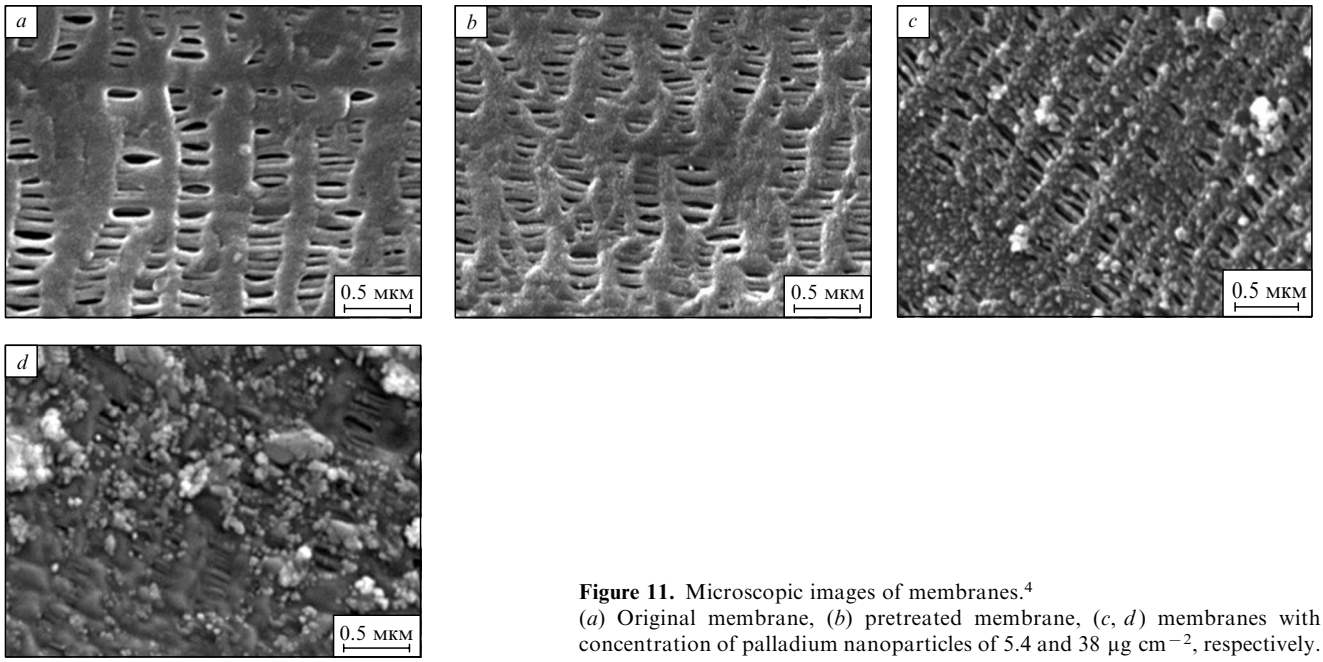


Figure 11. Microscopic images of membranes.[4]
(*a*) Original membrane, (*b*) pretreated membrane, (*c*, *d*) membranes with concentration of palladium nanoparticles of 5.4 and 38 μg cm^{-2}, respectively.

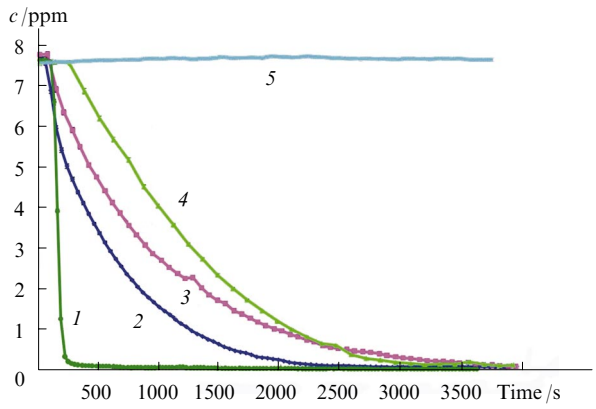


Figure 12. Dissolved oxygen concentration (*c*) *vs.* time for an experiment carried out in the dead-end mode of hydrogen supply to a laboratory catalytic membrane module; water flow rate: 20 (*1*), 13 (*2*), 9 (*3*) and 5 litre h^{-1}(*4*); (*5*) oxygen content for the case of helium supplied in place of hydrogen.[4]

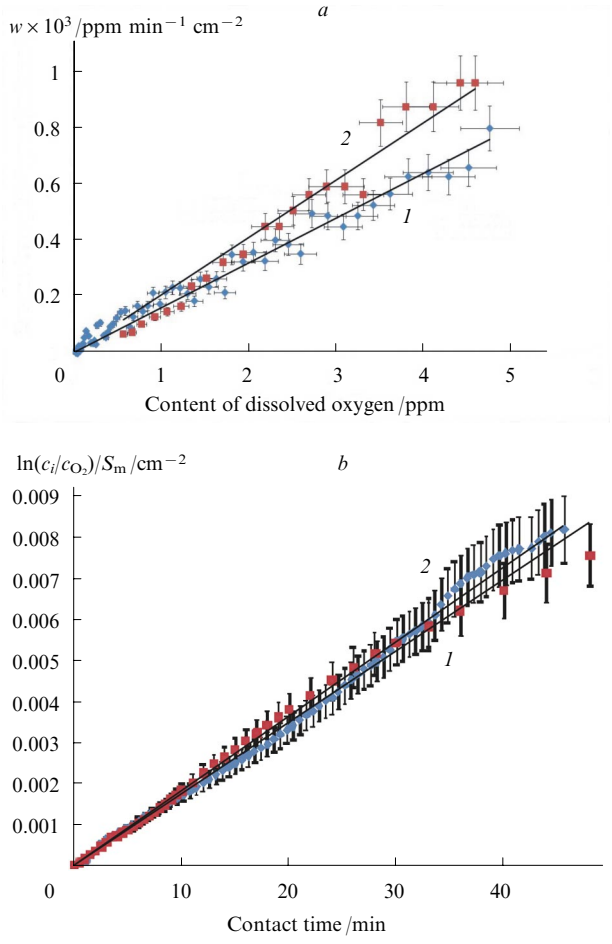


Figure 13. Kinetic curves of the removal of dissolved oxygen from water in a laboratory catalytic contactor/reactor.
(*a*) Rate of oxygen removal from water (*w*) *vs.* current concentration of oxygen; (*b*) logarithm of concentration of water-dissolved oxygen *vs.* contact time. Mode of metal deposition on the membrane: (*1*) continuous, (*2*) stepwise.

where the difference $c_{i+1} - c_i$ implies the change in the concentration in the period of $t_{i+1} - t_i$, S_m is the membrane geometrical surface area.

The dependences shown in Fig. 13 *a* are linear, *i.e.*, the rate of oxygen removal is indeed proportional to its concentration in a wide range of values; hence, the oxygen removal is a first-order reaction. Processing the kinetic dependences by a standard procedure (see Fig. 13 *b*) has shown that the linear dependence of the logarithm of concentration on time, which corresponds to the first order, describes the experimental results with the correlation coefficient virtually equal to unity. The rates of removal of dissolved oxygen achieved with the use of catalytic membranes prepared in different modes of palladium deposition coincided to a high degree of accuracy (see Fig. 13 *b*). Thus, in practice, one can use a method that appears to be most facile for a particular system. Note also the high efficiency of the method of oxygen removal proposed by Volkov *et al.*[4]

VI. Oxygen reduction in ion-exchange systems

As was mentioned above, ion exchangers serve as a sort of nanoreactors for controlled synthesis of metal nanoparticles. It seems quite natural to use nanocomposites synthesized based on them in the removal of oxygen from water.

1. Oxygen removal with the use of catalyst-modified ion-exchange membranes

Shi *et al.*[198] considered the processes of removal of dissolved oxygen from water tcatalyzed by palladium nanoparticles incorporated into a cation-exchange resin based on styrene cross-linked with divinylbenzene. The resin in its acidic form was loaded into the reactor (with the inner diameter of 28 mm and the length of 160 cm) to form a 62 cm thick bed. Due to the ion exchange process, the resin was transformed into its salt form (Pd^{2+}) and then Pd^{2+} was reduced to Pd^0 in a hydrogen flow. According to this method, the catalysts containing palladium nanoparticles with the concentration of 3.5 mass % and the average size of 27 nm were synthesized.

The dissolved oxygen was removed in two stages. First, hydrogen was dissolved in water in a saturator with ceramic packing; then water was fed to the catalytic packed-bed reactor for oxygen reduction with hydrogen. The concentration of dissolved oxygen of 10 μg kg^{-1} could be achieved when the experiment was continued for at least 30 min. Presumably, this was due to the fact that in the earlier stages of this process, the larger part of dissolved hydrogen was adsorbed on the catalyst active sites.[198]

The concentration of dissolved oxygen in water can be lowered down as a result of electrochemical reduction on the cathode. To accomplish this process, a bulk cathode packed with graphite (1.0–1.4 mm), nickel (0.6–0.85 mm) or copper (0.2–1.2 mm) particles was employed.[207–209] Among the listed cathode materials, copper demonstrated noticeable advantages. On the both sides of the cathode, cation-exchange membranes were placed. A crucial issue is that membranes should exhibit the maximum barrier properties (*i.e.*, the minimum permeability) with respect to molecular oxygen.

The water to be cleaned was supplied to the packed cathode on which dissolved oxygen was reduced, while molecular oxygen was generated on the anode. Due to

barrier properties of cation-exchange membranes, molecular oxygen did not reach the cathode but was disposed through the outlet channel. In laboratory studies[207] and pilot-plant tests,[208] the oxygen concentration in water could be reduced to 3 μg kg^{-1}. Presumably, the proposed method of electrochemical removal of oxygen from water can find its application in those cases where efficient portable devices for non-toxic removal of oxygen are needed.

However, for water with a reduced salt content, the efficiency of this method is low. To enhance the method, it was proposed to use cathodes packed with copper particles together with particles of a strong cation exchanger (in H^+- or Ca^{2+}-form).[209] The best results were exhibited by a resin that contained small particles and had a low degree of cross-linking. The oxygen concentration in distilled water with a low conductivity (0.003 mS cm^{-1}) was reduced from 8000 to 3 μg kg^{-1}.

2. Oxygen removal with the use of ion-exchange systems modified with active metal

When dissolved oxygen is to be absorbed from deionized water using nanocomposites composed of a chemically reactive metal and a sulfo cation exchange matrix, the following multistage redox-sorption process takes place: the diffusion of oxygen molecules through the pores of the ion-exchange matrix, the redox reaction between metal particles and oxygen which also involves the matrix counter-ions and, finally, the substitution of one counter-ion for another. Generally, the following transformations take place:[2]

$$4[RSO_3^-H^+]_zM_n^0 + zO_2 \longrightarrow 4[(RSO_3^-)_zM^{z+}]M_{n-1}^0 + 2zH_2O \quad (9)$$

Zero-valent metal is ionized, metal ions displace the hydrogen counter-ions located near the fixed groups of the ion-exchange matrix, while hydrogen counter-ions take part in the reaction of oxygen reduction. The reaction produces water molecules. Upon exhaustion of hydrogen counter-ions, the reaction produces metal oxides or hydroxides in the intermediate or final oxidation states.

The macrokinetics of redox sorbtion should be considered based on various assumptions. It can be assumed that the limiting stage is the redox reaction in the course of which the groups distributed throughout the matrix are transformed into the oxidized or reduced groups. In the case of instantaneous reaction, the process is controlled by the diffusion of the redox agent through the solution volume (the external diffusion kinetics) or through the sorbent bulk (the internal diffusion kinetics) to the interface.

In early studies (see, *e.g.*, Ref. 210) it was assumed that the diffusion kinetics of the absorption of redox agent is similar to the ion-exchange kinetics in ion exchangers. Hence, the mathematical description of the diffusion kinetics in nanocomposites and ion exchangers may be expected to be similar. However, this is not the case. The basic difference lies first of all in the mechanisms of these processes, which naturally results in a substantial difference in the mathematical description of their macrokinetics. Whereas in ion exchange, equivalent substitution of one ion for another ion takes place on functional groups, in contrast, upon sorption of oxidizing or reducing agents on nanocomposites, the majority of redox reactions are irreversible so that the active groups can be involved neither in repeated exchange nor in the further transfer of oxidizing or reducing agent molecules. The peculiarity of the diffusion process in the latter system is that it does not involve the oxygen molecule.

Yet another important peculiarity of the diffusion process accompanied by a redox reaction is the multistage mechanism of the electron transfer to produce a non-uniform spatial-temporal structure that consists of reaction products in different oxidation states. It is rare that all electrons are generated simultaneously. Usually a multistage reaction takes place, in intermediate stages of which the compounds in different oxidation states and electrons are simultaneously transferred through the sorbent. The intermediate products such as metal oxides with different oxidation states of the metal in metal/ion exchange composites can be sufficiently stable. Each stage has its own rate and propagates correspondingly throughout the sorbent. Apparently, this explains the presence of several redox zones (and boundaries between them) with individual diffusion coefficients of the redox agent.[211]

The proposed kinetic models of chemisorption processes partially consider these stages; their generalized analysis can be found in several publications, *e.g.*, Refs 2, 212–222.

When reacting with the oxidant, the active metal particles introduced into the ion-exchange matrix undergo certain modifications; as regards the effect on the total sorption rate, most significant is the gradual decrease in their size from a certain initial value to complete disappearance as a result of transition from the reduced state to one or another oxidation product. Moreover, besides the decrease in the reaction surface, some changes in the specific reaction rate are also probable.[32] With due regard to the latter, the physicochemical model of redox sorption of a molecular oxidant on metal/ion exchanger nanocomposites was constructed.[223, 224] The authors restricted their consideration to sorbents in the H^+-form with the metal content equivalent to the ion-exchange capacity (in this case, the metal oxidation can be considered as a single-stage reaction without taking into account the changes in the mechanism that accompany its evolution).

According to calculations, as the metal specific surface area increases due to a decrease in the initial size of nanoparticles (r_0), the rate of the chemical stage increases thus accelerating the overall sorption process, as evidenced from the dependence of the time necessary for the reaction to reach the degree of completion of 0.85 ($t_{0.85}$) on the initial radius of the metal particle (Fig. 14). The independence of

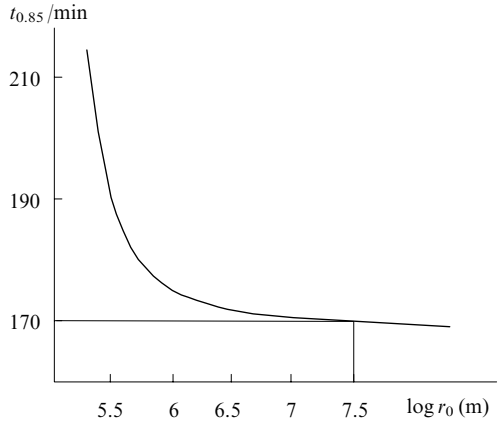


Figure 14. Time required to reach a 0.85 degree of process completion *vs.* the size of metal particles.[223]

the metal oxidation rate of the size of metal particles, which is illustrated by the invariance of $t_{0.85}$ for $-\log r_0 > 7.5$ ($r_0 < 0.32 \times 10^{-7}$ m), suggests that the oxygen sorption is limited by its internal diffusion (the system passes to the region of internal diffusion limitations).

Thus, based on model calculations, it was shown that with the increase in the degree of dispersion of metal particles in the nanocomposite, the oxygen sorption rate substantially increases due to the increase in the contact area between reacting particles. In this case, the process passes to the region of internal diffusion limitations.

3. Flow-through reactor

Figure 15 illustrates how the size and distribution of metal particles over a sorbent grain affect the form of the yield curve of sorption of water-dissolved oxygen in a flow-through reactor of the column type (filter). The analysis involving numerical calculations was carried out for a nanocomposite containing copper deposited in a single step to form spherical grains.[225] The increase in the metal surface with a decrease in the metal particle size was found to strongly affect the shape of the yield curve especially in its initial segment (see Fig. 15 *a*). This result is quite logical bearing in mind the fact that with the process evolution, the reaction front shifts to the grain centre. This leads to the complete transition of the system into the region of internal diffusion limitations. As the grain surface is enriched with metal and the linear distribution is transformed to parabolic one (see Fig. 15 *b*), the curve position changes, the efficiency of catalyst bed operation in the initial stage increases but the redox capacity is exhausted much faster (the capacity with respect to metal).

The practical value of a nanocomposite reactor is assessed by the period during which the oxygen concentration at the reactor outlet remains equal to zero, *i.e.*, is determined by the shape of the initial region of the yield curve. Based on results of calculations shown in Fig. 16, it can be concluded that the reaction efficiency increases as the metal degree of dispersion and concentration in the near-surface layer increase.

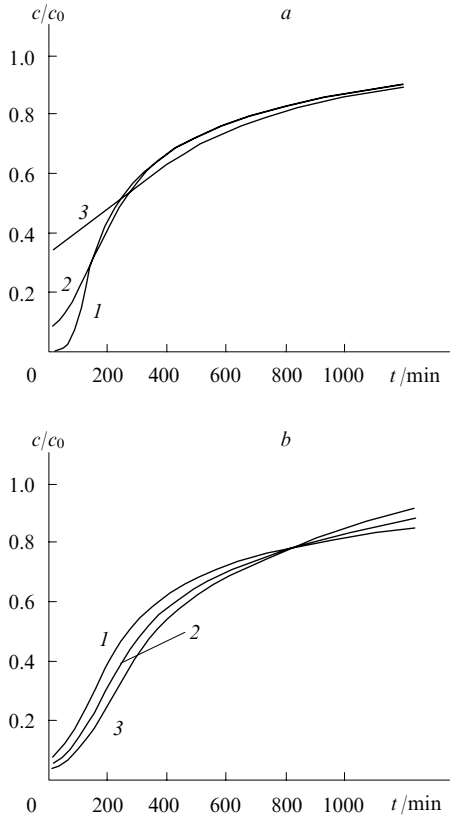


Figure 15. Effect of size (*a*) and distribution of metal particles over the sorbent grain (*b*) on the pattern of yield curve for redox sorption of molecular oxygen from water in a copper-packed bed of an electron ion exchanger.[225]
The bed height is 0.06 m, the solution flow rate is 10 m h^{-1}, the inlet oxygen concentration (c_0) is 0.26 mmol $litre^{-1}$; (*a*) r_0/μm: (*1*) 0.1, (*2*) 1, (*3*) 5; (*b*) distribution: (*1*) uniform, (*2*) linear, (*3*) parabolic; The form of the function is shown in the inset of Fig. 16.

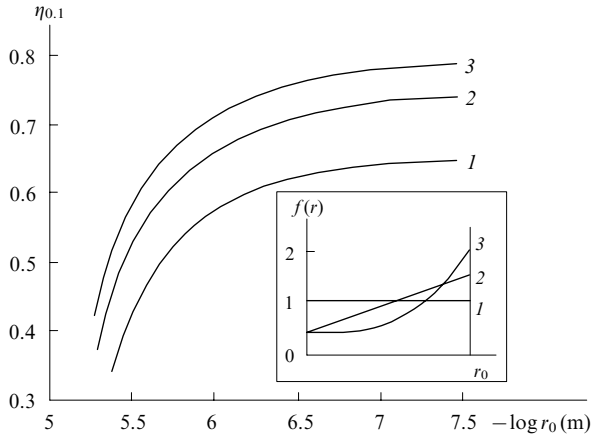


Figure 16. Effect of the copper grain size on the utilization factor of the redox capacity of the granular bed in an electron-ion exchanger.[225]
$\eta_{0.1}$ is redox-capacity utilization factor upon reaching the relative oxygen concentration at the outlet $c/c_0 = 0.1$; the bed height is 0.3 m, the solution flow rate is 18 m h^{-1}, the form of functions for the radial distribution of the metal over the grain (inset); distribution: (*1*) uniform, (*2*) linear, (*3*) parabolic.

Oxygen can be removed most efficiently in a two-step procedure, namely, by passing water successively through filters packed with $Cu^0 \cdot$KU-23 in the H^+-form and AV-17-8 in the SO_3^{2-}-form.[2]

4. Closed loop

When oxygen is removed from water contained in closed water loops, its concentration at the inlet of the redox filter varies. Figure 17 shows the changes in the oxygen concentration in the system equipped with a redox filter packed with $Cu^0 \cdot$KU-23 in the H^+-form with the capacity of 6.5 mg-equiv cm^{-3} with respect to metallic copper in a 100-litre closed water loop.

In 20 min after the activation of the redox filter, the oxygen concentration in the system decreases from 8 mg $litre^{-1}$ to 10 μg $litre^{-1}$. After this, the filter can be disconnected and activated again when the oxygen concentration in the system increases. Assuming that the filter utilization factor is 0.4, its capacity is 2.5 m^3 h^{-1} and the initial oxygen concentration is 0.1 mg $litre^{-1}$ (at this con-

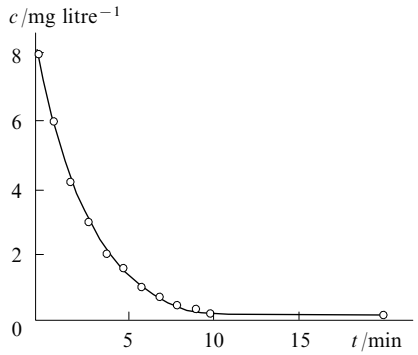


Figure 17. Variation of the oxygen concentration in a closed system due to operation of a redox filter packed with $Cu^0 \cdot$ KU-23 nanocomposite in the H^+-form.[2]
The bed height is 0.8 m, the bed cross-section is 7×10^{-2} m^2, the water flow rate is 0.5×10^{-2} m s^{-1}; the points are experimental data, the curve shows calculation results.

centration, it is recommended to activate the filter), then the time of filter operation is 5000 h.

Thus, metal(copper)/ion exchanger nanocomposites can be efficiently used as the redox sorbents of oxygen dissolved in water in order to produce high-purity water in flow-through and closed water systems.

* * *

Nanocomposite polymer catalytic membranes and ion exchangers are able to decrease the oxygen content in water down to the level required by modern industrial processes. The metal nanopartcles used therein play the dominating role in processes of oxygen removal from water. A high level of control over the properties of nanoparticles synthesized in various matrices has been achieved, which points to good prospects of nanocomposite materials in solving the problem of oxygen removal from various media.

This review was written with the partial financial support by the Russian Foundation of Basic Research (Project Nos 11-08-00174-a and 11-08-01083-a).

References

1. G Seo, T J Kim, S Lim, C H Ko, R Ryoo *Korean J. Chem. Eng.* **15** 611 (1998)
2. T A Kravchenko, L N Polyanskii, A I Kalinichev, D V Konev *Nanokompozity Metall/Ionoobmennik* (Metal/Ion exchanger Nanocomposites) (Moscow: Nauka, 2009)
3. *Ultra-Pure Water. Ultraclean Technology Handbook* Vol. 1 (Ed. T Ohmi) (West Conshohocken, PA: CRC Press, 1993)
4. V V Volkov, V I Lebedeva, I V Petrova, A V Bobyl, S G Konnikov, V I Roldughin, J van Erkel, G F Tereshchenko *Adv. Colloid Interface Sci.* **164** 144 (2011)
5. V V Volkov, I V Petrova, V I Lebedeva, V I Roldughin, G F Tereshchenko, in *Membranes for Membrane Reactors: Preparation, Optimization and Selection* (Eds A Basile, F Gallucci) (Singapore: Wiley, 2011) p. 531
6. V M Gryaznov *Dokl. Akad. Nauk SSSR* **189** 794 (1969) [a]
7. USSR P. 274092 (1964)
8. V M Gryaznov, M M Ermilova, L D Gogua, N V Orekhova, L S Morozova *Bull. Acad. Sci. USSR, Div. Chem. Sci.* **30** 672 (1981) [*Izv. Akad. Nauk SSSR, Ser. Khim.* 891 (1981)]
9. V M Gryaznov, N V Orekhova, in *Structured Catalysts and Reactors* (Eds A Cybulski, J A Moulijn) (New York: Marcel Dekker, 1997) p. 256
10. V M Gryaznov *Platinum Met. Rev.* **36** 70 (1992)
11. US P. 4132668 (1979)
12. US P. 4394294 (1983)
13. V M Gryaznov, O S Serebryannikova, Yu M Serov, M M Ermilova, A N Karavanov, A P Mischenko, N V Orekhova *J. Membr. Sci.* **77** 284 (1993)
14. V M Gryaznov, O S Serebryannikova, Yu M Serov, M M Ermilova, A N Karavanov, A P Mischenko, N V Orekhova *Appl. Catal. A* **96** 15 (1993)
15. I V J Vankelecom *Chem. Rev.* **102** 3779 (2002)
16. B M L Dioos, I V J Vankelecom , P A Jacobs *Adv. Synth. Catal.* **348** 1413 (2006)
17. *Metal–Polymer Nanocomposites* (Eds L Nicolais, G Carotenuto) (New York, N J: Wiley-Interscience, 2005)
18. S S Ozdemir, M G Buonomenna, E Drioli *Appl. Catal. A* **307** 167 (2006)
19. F Helfferich *Ion Exchange* (New York: McGraw-Hill, 1962)
20. H G Cassidy, K A Kun *Oxydation–Reduction Polymers* (*Redox Polymers*) (New York: Interscience, 1965)
21. A V Kozhevnikov *Elektronoionoobmenniki* (Electron Ion Exchangers) (Lenigrad: Khimiya, 1972)
22. A A Zagorodni *Ion Exchange Materials* (Amsterdam: Elsevier, 2007)
23. A D Pomogailo, A S Rozenberg, I E Uflyand *Nanochastitsy Metallov v Polimerakh* (Metal Nanoparticles in Polymers) (Moscow: Khimiya, 2000)
24. V I Roldughin *Russ. Chem. Rev.* **69** 821 (2000)
25. M C Daniel, D Astruc *Chem. Rev.* **104** 293 (2004)
26. I P Suzdalev *Nanotekhnologiya. Fizikokhimiya Nanoklasterov, Nanostruktur i Nanomaterialov* (Nanotechnology: Physical Chemistry of Nanoclusters, Nanostructures and Nanomaterials) (Moscow: URSS, 2005)
27. L A Dykman, V A Bogatyrev, S Yu Shchegolev, N G Khlebtsov *Zolotye Nanochastitsy. Sintez, Svoistva, Biomeditsinskoe Primenenie* (Gold Nanoparticles: Synthesis, Properties, Biomedical Applications) (Moscow: Nauka, 2008)
28. Yu I Petrov *Fizika Malykh Chastits* (Physics of Small Particles) (Moscow: Nauka, 1980)
29. O Daub, W Lange, C Reiner, L Kienle *Ber. Bunsen-ges. Phys. Chem.* **101** 753 (1997)
30. N Satoh, H Hasegawa, K Tsujii, K Kimura *J. Phys. Chem.* **98** 2143 (1994)
31. Y Takeuchi, T Ida, K Kimura *J. Phys. Chem. B* **101** 1322 (1997)
32. G B Sergeev *Nanokhimiya* (Nanochemistry) (Moscow: Moscow State University, 2007)
33. V V Zagorskii, S V Ivashko, V E Bochenkov, G B Sergeev *Nanostruct. Mater.* **12** 863 (1999)
34. S Tohno, M Itoh, H Takano *J. Aerosol Sci.* **25** S39 (1994)
35. S Tohno, M Itoh, S Aono, H Takano *J. Colloid Interface Sci.* **180** 574 (1996)
36. L Dimesso, S Humm, H Fuess, H Hahn *Ber. Bunsen-ges. Phys. Chem.* **101** 1750 (1997)
37. E D Shchukin, A V Pertsov, E A Amelina *Kolloidnaya Khimiya* (Colloid Chemistry) (Moscow: Vysshaya Shkola, 2004)
38. *Clusters and Colloids: from Theory to Applications* (Ed. G Schmid) (Weinheim: VCH, 1994)
39. *Nanoparticles and Nanostructured Films* (Ed. J H Fendler) (Weinheim: Wiley-VCH, 1998)
40. V I Roldughin *Rus. J. Phys. Chem.* **74** S522 (2000)
41. V I Roldughin *Fizikokhimiya Poverkhnosti* (Physical Chemistry of Surface) (Dolgoprudnyi: Intellekt, 2008)
42. N D Zhuravlev, V I Roldughin, A P Tikhonov *Kolloid. Zh.* **61** 325 (1999) [b]
43. R M Rioux, H Song, J D Hoefelmeyer, P Yang, G A Somorjai *J. Phys. Chem. B* **109** 2192 (2005)

44. H Song, R M Rioux, J D Hoefelmeyer, R Komor, K Niesz, M Grass, P D Yang, G A Somorjai *J. Am. Chem. Soc.* **128** 3027 (2006)
45. S M Humphrey, M E Grass, S E Habas, K Niesz, G A Somorjai, T D Tilley *Nano Lett.* **7** 785 (2007)
46. Y Zhang, M E Grass, S E Habas, F Tao, T Zhang, P Yang, G A Somorjai *J. Phys. Chem. C* **111** 12243 (2007)
47. A Gniewek, J J Ziolkowski, A M Trzeciak, L Kepinsk *J. Catal.* **239** 272 (2006)
48. H Tsunoyama, H Sakurai, Y Negishi, T Tsukuda *J. Am. Chem. Soc.* **127** 9374 (2005)
49. A Miyazaki, I Balint, Y Nakano *J. Nano Res.* **5** 69 (2003)
50. M A R Meier, M Filali, J-F Gohy, U S Schubert *J. Mater. Chem.* **16** 3001 (2006)
51. A B R Mayer, J E Mark *Colloid Polym. Sci.* **275** 333 (1997)
52. I P Beletskaya, A N Kashin, A E Litvinov, V S Tyurin, P M Valetsky, G van Koten *Organometallics* **25** 54 (2006)
53. H Lee, S E Habas, S Kweskin, D Butcher, G A Somorjai, P D Yang *Angew. Chem., Int. Ed.* **45** 7824 (2006)
54. K M Bratlie, H Lee, K Komvopoulos, P Yang, G A Somorjai *Nano Lett.* **7** 3097 (2007)
55. R Narayanan, M A El-Sayed *Top. Catal.* **47** 15 (2008)
56. S Shirinita, T Takasaki, T Kamegawa, K Mori, H Yamashita *Top. Catal.* **53** 218 (2010)
57. E Horvárth, R Puskás, R Remiás, M Mohl, A Kukovecz, Z Kónya, I Kiricsi *Top. Catal.* **52** 1242 (2009)
58. R M Roix, H Song, M Grass, S Habas, K Niesz, J D Hoelmeyer, P Yang, G A Samorjai *Top. Catal.* **39** 167 (2006)
59. I Ichinose, H Senzu, T Kunitake *Chem. Mater.* **9** 1296 (1997)
60. W Yan, S M Mahurin, S H Overbury, S Dai *Top. Catal.* **39** 199 (2006)
61. G G Wildgoose, C E Banks, R G Compton *Small* **2** 182 (2006)
62. M Endo, T Hayashi, Y A Kim, M Terrones, M S Dresselhaus *Philos. Trans. R. Soc. London, Ser. A* **362** 2223 (2004)
63. P Serp, M Corrias, P Kalck *Appl. Catal. A* **253** 337 (2003)
64. I Kvande, S T Briskeby, M Tsypkin, M Rønning, S Sunde, R Tunold, D Chen *Top. Catal.* **45** 81 (2007)
65. D V Bavykin, A A Lapkin, P K Plucinski, L Torrente-Murciano, J M Friedrich, F C Walsh *Top. Catal.* **39** 151 (2006)
66. K Lee, J Zhang, H Wang, D P Wilkinson *J. Appl. Electrochem.* **36** 507 (2006)
67. J Wang, G Yin, Y Shao, Z Wang, Y Gao *J. Phys. Chem. C* **112** 5784 (2008)
68. S Takenaka, H Umebayashi, E Tanabe, H Matsune, M Kishida *J. Catal.* **245** 392 (2007)
69. S Takenaka, Y Orita, H Matsune, E Tanabe, M Kishida *J. Phys. Chem. C* **111** 7748 (2007)
70. S Takenaka, H Matsumori, T Arike, H Matsune, M Kishida *Top. Catal.* **52** 731 (2009)
71. J Whitesides, D Agler, R Anders *Nanotechnology in the Nearest Decade. Forecast for the Research Areas* (Eds M K Roko, R S Williams, P Alivisatos) (Dordrecht: Kluwer Academic, 2001)
72. S Kéki, J Török, G Deák, L Daróczi, M Zsuga *J. Colloid Interface Sci.* **229** 550 (2000)
73. M-K Kim, Y-M Jeon, W S Jeon, H J Kim, S G Hong, C G Park, K Kim *Chem. Commun.* 667 (2001)
74. E Hao, T Lian *Chem. Mater.* **12** 3392 (2000)
75. P Yang, W Zhang, Y Du, X Wang *J. Mol. Catal. A* **260** 4 (2006)
76. R M Crooks, M Q Zhao, L Sun, V Chechik, L K Yeung *Acc. Chem. Res.* **34** 181 (2001)
77. X H Peng, Q M Pan, G L Rempel *Chem. Soc. Rev.* **37** 1619 (2008)
78. W Huang, J N Kuhn, C K Tsung, Y Zhang, S E Habas, P Yang, G A Somorjai *Nano Lett.* **8** 2027 (2008)
79. L Wu, B-L Li, Y-Y Huang, H-F Zhou, Y-M He, Q-H Fan *Org. Lett.* **8** 3605 (2006)
80. R M Crooks, M Zhao, L Sun, V Chechik, L K Yeung *Acc. Chem. Res.* **34** (2009)
81. H Giersig, P Mulvaney *Langmuir* **9** 3408 (1993)
82. M Brust, M Walker, D Bethell, D J Schiffrin, R J Whyman *J. Chem. Soc., Chem. Commun.* 801 (1994)
83. M Brust, J Fink, D Bethell, D J Schiffrin, C J Kiely, R J Whyman *J. Chem. Soc., Chem. Commun.* 1165 (1995)
84. R H Terrill, T A Postlethwait, C Chen, C Poon, A Terzis, A Chen, J E Hutchinson, M R Clark, G Wingnall, J D Londono, R Superfine, M Falvo, C S Johnson, E T Samulski, R W Murray *J. Am. Chem. Soc.* **117** 12537 (1995)
85. D V Leff, P C Ohara, J R Heath, W M Gelbart *J. Phys. Chem.* **99** 7036 (1995)
86. M J Hostetler, J J Stokes, R W Murray *Langmuir* **12** 3604 (1996)
87. R L Whetten, J T Khoury, M M Alvarez, S Murphy, I Vezmar, Z L Wang, P W Stephens, C L Cleveland, W D Luedtke, U Landman *Adv. Mater.* **8** 428 (1996)
88. A Badia, S Singh, L Demers, L Cuccia, G R Brown, R B Lennox *Chem. – Eur. J.* **2** 359 (1996)
89. S R Johnson, S D Evans, S W Mahon, A Ulman *Langmuir* **13** 51 (1997)
90. G V Lisichkin, A Yu Fadeev, A A Serdan, P N Nesterenko, P G Mingalev, D B Furman *Khimiya Privitykh Soedinenii* (The Chemistry of Graft Compounds) (Moscow: Fizmatlit, 2003)
91. S A Harfenist, Z L Wang, M M Alvarez, I Vezmar, R L Whetten *J. Phys. Chem.* **100** 13904 (1996)
92. J R Heath, C M Knobler, D W Leff *J. Phys. Chem. B* **101** 189 (1997)
93. K W Sarathy, G U Kulkarni, C N R Rao *Chem. Commun.* 537 (1997)
94. A Taleb, C Petit, M P Pileni *Chem. Mater.* **9** 950 (1997)
95. S Y Kang, K Kim *Langmuir* **14** 226 (1998)
96. Y P Sun, J E Riggs, H W Rollins, R Guduru *J. Phys. Chem. B* **103** 77 (1999)
97. M Alvarez, J Khoury, T Schaaf, M Shafigullin, I Vezmar, R Whetten *Chem. Phys. Lett.* **266** 91 (1997)
98. M J Hostetler, J E Wingate, C-J Zhong, J E Harris, R W Vachet, M R Clark, J D Londono, S J Green, J J Stokes, G D Wignall, G L Glish, M D Porter, N D Evans, R W Murray *Langmuir* **14** 17 (1998)
99. C A Bauer, F Stellacci, J W Perry *Top. Catal.* **47** 32 (2008)
100. I Chorkendorf, Kh Naimantsvedrait *Sovremennyi Kataliz i Khimicheskaya Kinetika* (Modern Catalysis and Chemical Kinetics) (Dolgoprudnyi: Intellekt, 2010)
101. O V Dement'eva, M A Filippenko, M E Kartseva, V M Rudoi *Kolloid. Zh.* **71** 575 (2009) [b]
102. B G Ershov, E V Abkhalimov, V V Vysotskii, V I Roldughin *Kolloid Zh.* **72** 171 (2010) [b]
103. S E Habas, H Lee, V Radmilovic, G A Somorjai, P Yang *Nature Mater.* **6** 692 (2007)
104. E V Shevchenko, D V Talapin, A L Rogach, A Kornowski, M Haase, H Weller *J. Am. Chem. Soc.* **124** 11480 (2002)
105. E V Shevchenko, D V Talapin, N A Kotov, S O'Brien, C B Murray *Nature (London)* **439** 55 (2006)
106. A Beck, A Horváth, Z Schay, G Stefler, Z Koppány, I Saju, O Geszti, L Guszci *Top. Catal.* **44** 115 (2007)
107. L Prati, A Villa, C Campione, P Spontoni *Top. Catal.* **44** 319 (2007)
108. A Rogach, A Susha, F Caruso, G Sukhorukov, A Kornowski, S Kershaw, H Möhwald, A Eychmüller, H Weller *Adv. Mater.* **12** 333 (2000)
109. Y Xia, B Gates, Y Yin, Y Lu *Adv. Mater.* **12** 693 (2000)
110. H Hofmeister, P-T Miclea, M Steen , W Mörke, H Drevs *Top. Catal.* **46** 11 (2007)
111. S J Tauster, S C Fung, R L Garten *J. Am. Chem. Soc.* **100** 170 (1978)

112. K Hayek, M Fuchs, B Klotzer, W Reichl, G Rupprechter *Top. Catal.* **13** 55 (2000)
113. *Fine Particles — Synthesis, Characterization and Mechanisms of Growth*. (Ed. T Sugimoto) (New York: Marcel Dekker, 2000)
114. M J Kim, E Matijevic *J. Mater. Res.* **6** 840 (1991)
115. S Iijima, M Ichikawa *J. Catal.* **94** 313 (1985)
116. A K Datye, N J Long *Ultramicroscopy* **25** 203 (1988)
117. P L Gai, K Kourtakis, E D Boyes *Catal. Lett.* **102** 17 (2005)
118. Z-J Jiang, C-Y Liu, L-W Sun *J. Phys. Chem. B* **109** 1730 (2005)
119. C W Chen, M Q Chen, T Serizawa, M Akashi *Adv. Mater.* **10** 1122 (1998)
120. M E Kartseva, O V Dement'eva, M A Filippenko, V M Rudoi *Kolloid. Zh.* **73** 334 (2011) [b]
121. Y D Yin, R M Rioux, C K Erdonmez, S Hughes, G A Somorjai, A P Alivisatos *Science* **304** 711 (2004).
122. M Haruta, T Kobayashi, H Sano, N Yamada *Chem. Lett.* 405 (1987)
123. M Haruta, N Yamada, T Kobayashi, S Ijima *J. Catal.* **115** 301 (1989)
124. G J Hutchings, S Carrettine, P Landon, J K Edwarda, D Enache, D W Knight, Y-J Xu, A F Carley *Top. Catal.* **38** 223 (2006)
125. F Moreau, G C Bond *Top. Catal.* **44** 95 (2007)
126. J C Fierro-Gonzalez, J Guzman, B C Gates *Top. Catal.* **44** 103 (2007)
127. U Landman, B Yoon, C Zhang, U Heiz, M Arenz *Top. Catal.* **44** 145 (2007)
128. C D Pina, E Falletta, M Rossi *Top. Catal.* **44** 325 (2007)
129. T V W Janssens, B S Clausen, B Hvolbæk, H Falsig, C H Christensen, T Bligaard, J K Nørskov *Top. Catal.* **44** 15 (2007)
130. J C McPherson, D T Thompson *Top. Catal.* **52** 743 (2009)
131. V V Pushkarev, Z Zhu,, K An, A Hervier, G A Somorjai *Top. Catal.* **55** 1257 (2012)
132. A Benedetti, G Fagherazzi, F Pinna, G Rampazzo, M Selva, G Strukul *Catal. Lett.* **10** 215 (1991)
133. R L Augustine, S T O'Leary *J. Mol. Catal. A: Chem.* **95** 277 (1995)
134. J A A Van Den Tillaart, B F M Kuster, G B Marin *Catal. Lett.* **36** 31 (1996)
135. S Mukerjee, J J McBreen *Electroanal. Chem.* **448** 163 (1998)
136. J Le Bars, U Specht, J S Bradley, D G Blackmond *Langmuir* **15** 7621 (1999)
137. L Piccolo, C R Henry *J. Mol. Catal. A: Chem.* **167** 18 (2001)
138. Y Li, X M Hong, D M Collard, M A El-Sayed *Org. Lett.* **2** 2385 (2000)
139. G A Samorjai, Y Li *Top. Catal.* **53** 832 (2010)
140. B Hammer *Top. Catal.* **37** 3 (2006)
141. R Narayanan, M A El-Sayed *J. Am. Chem. Soc.* **125** 8340 (2003)
142. R Narayanan, M A El-Sayed *Langmuir* **21** 2027 (2005)
143. H Topsøe *J. Catal.* **216** 155 (2003)
144. *Handbook of Heterogeneous Catalysis* (Eds G Ertl, H.Knözinger, J Weitkamp) (Weinheim: VCH, 1997)
145. J W Niemantsverdriet *Spectroscopy in Catalysis* (Weinheim: Wiley-VCH, 2000)
146. R Prins, D C Koningsberger *X-Ray Absorption: Principles, Applications, Techniques of EXAFS, SEXAFS, and XANES* (New York: Wiley, 1998)
147. J M Thomas, G A Somorjai *Top. Catal.* **8** 1 (1999)
148. B M Weckhuysen *Chem. Commun.* 97 (2002)
149. *In-Situ Spectroscopy in Heterogeneous Catalysis* (Ed. J F Haw) (Weinheim: Wiley-VCH, 2002)
150. Yu Suchorski, W Drachsel *Top. Catal.* **46** 201 (2007)
151. A M Molenbroek, S Helveg, H Topsøe, B S Clausen *Top. Catal.* **52** 1303 (2009)
152. G A Somorjai, J Y Park *Top. Catal.* **49** 126 (2008)
153. V I Roldughin *Russ. Chem. Rev.* **73** 115 (2004)
154. A M Contreras, J Grunes, X-M Yan, A Liddle, G A Somorjai *Top. Catal.* **39** 123 (2006)
155. N T Wilton, B Berton, R Bronstein, H-P Hentze, M Antonietti *Adv. Mater.* **11** 1014 (1999)
156. Ch-W Chen, M-Q Chen, Q Serizawa, M Akashi *Chem. Commun.* 831 (1998)
157. I V J Vankelecom, P A Jacobs *Catal. Today* **56** 147 (2000)
158. K Mallick, M J Witcomb, A Dinsmore, M S Scurrel *J. Mater. Sci.* **41** 1733 (2006)
159. S W Huang, K G Neoh, E T Kang, H S Hanb, K L Tanb *J. Mater. Chem.* **8** 1743 (1998)
160. R Diaz-Ayala, R Raptis, C R Cabrera *Rev. Adv. Mater. Sci.* **10** 375 (2005)
161. D M Dotzauer, J Dai, L Sun, M L Bruening *Nano Lett.* **6** 2268 (2006)
162. S Kidambi, M L Bruening *Chem. Mater.* **17** 301 (2005)
163. A Houdayer, R Schneider, D Billaud, J Ghanbaja, J Lambert *Appl. Organomet. Chem.* **19** 1239 (2005)
164. S Ziegler, J Theis, D Fritsch *J. Membr. Sci.* **187** 71 (2001)
165. M M Demir, M A Gulgun, Y Z Menceloglu, B Erman, S S Abramchuk, E E Makhaeva, A R Khokhlov, V G Matveeva, M G Sulman *Macromolecules* **37** 1787 (2004)
166. Y Li, E Boone, M A El-Sayed *Langmuir* **18** 4921 (2002)
167. N A Dhas, H Cohen, A Gedanken *J. Phys. Chem. B* **101** 6834 (1997)
168. T Teranishi, M Miyakees *Chem. Mater.* **11** 3414 (1999)
169. G Bengtson, H Scheel, J Theis, D Fritsch *Chem. Eng. J.* **85** 303 (2002)
170. G Bengtson, M Oehring, D Fritsch *Chem. Eng. Proc.* **43** 1159 (2004)
171. B M Sergeev, M V Kiryukhin, F N Bakhov, V G Sergeev *Vestn. Mosk. Univ., Ser. 2, Khim.* **42** 308 (2001) [c]
172. T A Kravchenko, N V Sotskaya, D V Konev, S V Peshkov. *Zh. Fiz. Khim.* **78** 1858 (2004) [d]
173. T A Kravchenko, M Yu Chaika, E V Bulavina, A V Glotov, A B Yaroslavtsev *Dokl. Akad. Nauk* **433** 55 (2010) [a]
174. S A Lilin, A V Balmasov, V I Parfenyuk, in *Proceedings of the 8th International Frumkin Symposium on Kinetics of Electrode Processes, Moscow, 2005* p. 290
175. G F Mills, B N Dickinson *Ind. Eng. Chem.* **41** 2842 (1949)
176. Yu A Tarasenko, I P Gerasimyuk, V F Lapko, V D Khavryuchenko *Ukr. Khim. Zh.* **72** 89 (2006) [e]
177. Yu A Tarasenko, G V Reznik, A A Bagreev, A A Lysenko *Zh. Fiz. Khim.* **67** 2333 (1993) [d]
178. I V Vol'f, A V Romanov *Sorbts. Khromatogr. Protsessy* **6** 1318 (2006)
179. I V Vol'f, M A Sinyakova *Sorbts. Khromatogr. Protsessy* **5** 415 (2005)
180. A S Podshivalov, T S Sokolova, in *Tezisy Dokladov Oblastnoi Konferentsii Molodykh Uchenykh i Studentov 'Problemy Khimii i Ekologii'* (Abstracts of Reports of the Regional Conference of Young Scientists and Students 'Problems of Chemistry and Ecology', Perm, 2000) p. 51
181. M J DeMarco, A K SenGupta, J E Greenleaf *Water Res.* **37** 164 (2003)
182. N M Kruglikova, A B Pashkov, A F Chetverikov *Plastmassy* (Plastic Materials) (Moscow: Khimiya, 1970)
183. USSR P. 232499; *Byull. Izobret.* (1) (1969)
184. V V Samonin, N F Fedorov *Zh. Prikl. Khim.* **70** 51 (1997) [f]
185. USSR P. 654623; *Byull. Izobret.* (12) 106 (1979)
186. V Z Radkevich, Yu G Egizarov *Zh. Prikl. Khim.* **75** 1673 (2002) [f]
187. JP P. 60135434 (1985)
188. N P Berezina, A A-R Kubaisi, I A Stenina, R V Smolka, S V Timofeev *Membrany* (32) 48 (2006)
189. W Hsing-Lin, L Wenguang, Q X Jia, E Akhadov *Chem. Mater.* **19** 520 (2007)
190. C A Novikova, A B Yaroslavtsev *Sorbts. Khromatogr. Protsessy* **8** 887 (2008)

191. H W Rollins, F Lin, J Johnson, J-J Ma, J-T Liu, M-H Tu, D D DesMarteau, V-P Sun *Langmuir* **16** 8031 (2000)
192. B I Podlovchenko,V N Andreev *Russ. Chem. Rev.* **71** 837 (2002)
193. F Wiesler *Ultrapure Water* **5**–**6** 27 (1996)
194. S W Huang, K G Neoh, E T Kang, H S Hanb, K L Tanb *J. Mater. Chem.* **8** 1743 (1998)
195. EP P. 0145262 (1985)
196. K Li, I Chua, W J Ng, W K Teo *Chem. Eng. Sci.* **50** 3547 (1995)
197. X Tan, K Li *Chem. Eng. Sci.* **55** 1213 (2000)
198. W Shi, C Cui, L Zhao, Sh Yu, X Yun *Front. Chem. Eng. China* **3** (1) 107 (2009)
199. M Kralik, A Biffis *J. Mol. Catal. A: Chem.* **177** 113 (2001)
200. M S Gross, M L Pisarello, K A Pierpauli, C A Querini *Ind. Eng. Chem. Res.* **49** 81 (2010)
201. NL P. 1023364 (2004)
202. R van der Vaart, B Hafkamp, P J Koele, M Querreveld, A E Jansen, V V Volkov, V I Lebedeva, V M Gryaznov *Ultrapure Water* **18** 27 (2001)
203. V I Lebedeva, V M Gryaznov, I V Petrova, V V Volkov, G F Tereshchenko, E I Shkol'nikov, L M Plyasova, D I Kochubey, R van der Vaart, E L D van Soest-Vercammen *Kinet. Catal.* **47** 864 (2006)
204. R van der Vaart, I Petrova, V Lebedeva, V Volkov, D Kochubey, G Tereshchenko *Desalination* **199** 424 (2006)
205. R van der Vaart, V I Lebedeva, I V Petrova, L M Plyasova, N A Rudina, D I Kochubey, G F Tereshchenko, V V Volkov, J van Erkel *J. Membr. Sci.* **299** 38 (2007)
206. V V Volkov, I V Petrova, V I Lebedeva, L M Plyasova, N A Rudina, J van Erkel, R van der Vaart, G F Tereshchenko, in *Nanoscience: Colloidal and Interfacial Aspects* (Ed. V M Starov) (New York: Taylor and Francis, 2011) p. 1173
207. K Vuorilehto, A Tamminen, S Ylasaari *J. Appl. Electrochem.* **25** 973 (1995)
208. A Tamminen, K Vuorilehto, S Ylasaari *J. Appl. Electrochem.* **26** 113 (1996)
209. A Tamminen, K Vuorilehto *J. Appl. Electrochem.* **27** 1095 (1997)
210. H Gregor, M Beltzer *J. Polym. Sci.* **53** 125 (1961)
211. T A Kravchenko, I V Aristov, in *Ion Exchange* (Eds D Muraviev, V Gorshkov, A Warshawsky) (New York, Basel: Marsel Dekker, 2000) p. 691
212. Yu A Kokotov, P P Zolotarev, G E El'kin *Teoreticheskie Osnovy Ionnogo Obmena. Slozhnye Ionoobmennye Sistemy* (Theoretical Foundations of Ion Exchange. Complex Ion-exchange Systems) (Leningrad: Nauka, 1989)
213. Yu P Znamenskii, N V Bychkov *Kinetika Ionoobmennykh Protsessov* (Kinetics of Ion-exchange Processes) (Obninsk: Printer, 2000)
214. F Helfferich *J. Phys. Chem.* **69** 1178 (1965)
215. N I Nikolaev *Kinet. Katal.* **9** 870 (1968) [g]
216. M Nativ, S Goldstein, G Schmuckler *J. Inorg. Nucl. Chem.* **37** 1951 (1975)
217. G Schmuckler *React. Polym.* **2** 103 (1984)
218. V A Kuz'minykh, T A Kravchenko, N A Kalyadina *Zh. Fiz. Khim.* **71** 2211 (1997) [d]
219. A I Kalinitchev *Ion Exchange* (Eds D Muraviev, V Gorshkov, A Warshawsky) (New York, Basel: Marsel Dekker, 2000)
220. T A Kravchenko, L A Shinkevich *Zh. Fiz. Khim.* **60** 2599 (1986) [d]
221. L A Shinkevich, V G Zadorozhnii, T A Kravchenko, N V Sotskaya *Zh. Fiz. Khim.* **60** 2601 (1986) [d]
222. L A Shinkevich, T A Kravchenko, A I Kalinichev, N V Sotskaya *Zh. Fiz. Khim.* **63** 2063 (1989) [d]
223. D V Konev, T A Kravchenko, A I Kalinichev, V A Krysanov *Zh. Fiz. Khim.* **81** 320 (2007) [d]
224. S V Peshkov, D V Konev, E S Kipriyanova, T A Kravchenko, A I Kalinichev *Zh. Fiz. Khim.* **85** 1612 (2011) [d]
225. D V Konev, T A Kravchenko, A I Kalinichev, E S Kipriyanova *Zh. Fiz. Khim.* **83** 948 (2009) [d]

[a] — *Dokl. Phys. Chem. (Engl. Transl.)*
[b] — *Colloid. J. (Engl. Transl.)*
[c] — *Moscow Univ. Chem. Bull. (Engl. Transl.)*
[d] — *Russ. J. Phys. Chem., Ser. A (Engl. Transl.)*
[e] — *Ukr. Chem. J. (Engl. Transl.)*
[f] — *Russ. J. Appl. Chem. (Engl. Transl.)*
[g] — *Kinet Catal. (Engl. Transl.)*